

# Accepted Manuscript

Computer-assisted design, synthesis, binding and cytotoxicity assessments of new 1-(4-(aryl(methyl)amino)butyl)-heterocyclic sigma 1 ligands

Daniele Zampieri, Luciano Vio, Maurizio Fermeglia, Sabrina Pricl, Bernhard Wünsch, Dirk Schepmann, Maurizio Romano, Maria Grazia Mamolo, Erik Laurini



PII: S0223-5234(16)30478-0

DOI: [10.1016/j.ejmech.2016.06.001](https://doi.org/10.1016/j.ejmech.2016.06.001)

Reference: EJMECH 8662

To appear in: *European Journal of Medicinal Chemistry*

Received Date: 4 April 2016

Revised Date: 30 May 2016

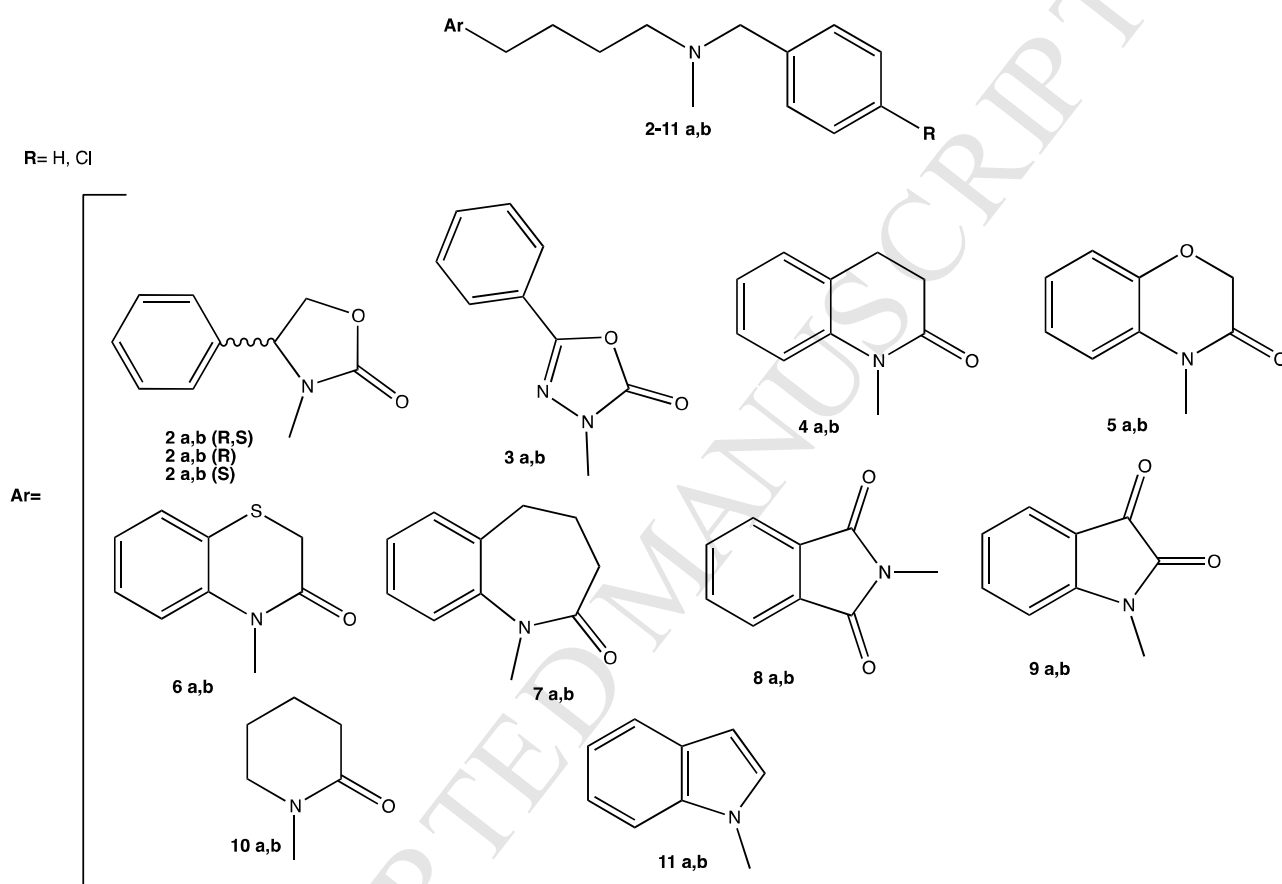
Accepted Date: 1 June 2016

Please cite this article as: D. Zampieri, L. Vio, M. Fermeglia, S. Pricl, B. Wünsch, D. Schepmann, M. Romano, M.G. Mamolo, E. Laurini, Computer-assisted design, synthesis, binding and cytotoxicity assessments of new 1-(4-(aryl(methyl)amino)butyl)-heterocyclic sigma 1 ligands, *European Journal of Medicinal Chemistry* (2016), doi: 10.1016/j.ejmech.2016.06.001.

This is a PDF file of an unedited manuscript that has been accepted for publication. As a service to our customers we are providing this early version of the manuscript. The manuscript will undergo copyediting, typesetting, and review of the resulting proof before it is published in its final form. Please note that during the production process errors may be discovered which could affect the content, and all legal disclaimers that apply to the journal pertain.

## Graphical Abstract

New 1-(4-(aryl(methyl)amino)butyl)-heterocyclic derivatives were designed and synthesized in order to evaluate their affinity towards  $\sigma$  receptors by radioligand binding assays. Moreover, in order to investigate their cytotoxic activity, a functional assay was performed.



Some of these derivatives showed a remarkable affinity and selectivity towards  $\sigma_1$  receptors and an interesting cytotoxic profile.

# Computer-assisted design, synthesis, binding and cytotoxicity assessments of new 1-(4-(aryl(methyl)amino)butyl)-heterocyclic sigma 1 ligands.

Daniele Zampieri<sup>a\*</sup>, Luciano Vio<sup>a†</sup>, Maurizio Fermeglia<sup>b</sup>, Sabrina Prict<sup>bc\*</sup>, Bernhard Wünsch<sup>d</sup>, Dirk Schepmann<sup>d</sup>, Maurizio Romano<sup>e</sup>, Maria Grazia Mamolo<sup>a#</sup>, Erik Laurini<sup>b#</sup>

<sup>a</sup> Department of Chemistry & Pharmaceutical Sciences, Piazzale Europa 1, University of Trieste, 34127 Trieste, Italy

<sup>b</sup> Molecular Simulation Engineering (MOSE) Laboratory, DEA, Piazzale Europa 1, University of Trieste, 34127 Trieste, Italy

<sup>c</sup> National Interuniversity Consortium for Material Science and Technology (INSTM), Research Unit MOSE-DEA, University of Trieste, Trieste - Italy

<sup>d</sup> Department of Pharmaceutical and Medicinal Chemistry, Corrensstrasse 48, University of Münster, 48149 Münster, Germany.

<sup>e</sup> Department of Life Sciences, Via Valerio 28/1, University of Trieste, 34127 Trieste, Italy

<sup>†</sup> "This work is dedicated to the fond memory of Prof. Luciano Vio, colleague and friend, unexpectedly deceased on May 5, 2016."

---

**Abstract.** In this work we applied a blend of computational and synthetic techniques with the aim to design, synthesize, and characterize new  $\sigma_1$  receptor ( $\sigma_1R$ ) ligands. Starting from the structure of previously reported, high-affinity benzoxazolone-based  $\sigma_1$  ligands, the three-dimensional homology model of the  $\sigma_1R$  was exploited for retrieving the molecular determinants to fulfill the optimal pharmacophore requirements. Accordingly, the benzoxazolone moiety was replaced by other heterocyclic scaffolds, the relevant conformational space in the  $\sigma_1R$  binding cavity was explored, and the effect on  $\sigma_1R$  binding affinity was ultimately assessed. Next, the compounds designed *in silico* were synthesized, and their affinity and selectivity toward  $\sigma_1$  and  $\sigma_2$  receptors were tested. Finally, a representative series of best  $\sigma_1R$  binders were assayed for cytotoxic activity on the SH-SY5Y human neuroblastoma cell line. Specifically, the new 4-phenyloxazolidin-2-one derivatives **2b** (i.e., (R)-**2b** and (S)-**2b**) emerged as potential leads for further development as  $\sigma_1R$  agents, as they were found endowed with the highest  $\sigma_1R$  affinity ( $K_{i\sigma_1}$  values in the range 0.95-9.3 nM), and showed minimal cytotoxic levels exhibited in the selected, cell-based test, in line with a  $\sigma_1R$  agonist behavior.

*Keywords:* sigma receptors; binding affinity; cytotoxicity; molecular modeling.

\*Corresponding author; Phone: +39 040 5587858; e-mail: [dzampieri@units.it](mailto:dzampieri@units.it); Phone: +39 040 5583750; e-mail: [sabrina.pricl@di3.units.it](mailto:sabrina.pricl@di3.units.it)

*#These authors contributed equally to this work*

## Introduction

After their initial misclassification as an opioid receptor subtype [1], sigma receptors ( $\sigma$ -Rs) actually represent a non-opioid, non-phencyclidine but haloperidol-sensitive receptor family [2]. To date, at least two distinct  $\sigma$ -Rs subtypes - designated as  $\sigma_1$  and  $\sigma_2$  [3] - have been pharmacologically characterized [4-6]. The amino acid sequence of the  $\sigma_1$  receptor ( $\sigma_1$ R) subtype was determined by purification and cloning from several animal species including man. Interestingly, this receptor shows no homology with any mammalian protein, whilst it exhibits significant homology (30%) with sterol C<sub>8</sub>- C<sub>7</sub> isomerase from fungi [7,8]. The  $\sigma_1$ R has been associated with many diseases including stroke, cocaine addiction, pain, cancer, and neurodegenerative pathologies [9].

On the other hand, the  $\sigma_2$  receptor subtype has not been cloned yet, although its molecular weight has been determined as approximately 21.5 kDa. [7] It has been proposed that this  $\sigma$ -R subtype is involved in cellular apoptotic response [10,11], and in the release of Ca<sup>2+</sup> through an IP<sub>3</sub>-independent manner [12-14].

To date, neither  $\sigma_1$ R endogenous ligands have been definitively established [15], nor the role of all  $\sigma_1$ R ligands has been unequivocally established in terms of their agonistic or antagonistic receptor activity [9]. Ligands displaying preferential affinity for the  $\sigma_1$ R subtype - and currently classified as  $\sigma_1$ R agonists - are dextrorotatory benzomorphans such as (+)-pentazocine and (+)-N-allylnormetazocine (NANM, aka SKF-10,047), whereas haloperidol (categorized as  $\sigma_1$ R antagonist) and 1,3-di-(2-tolyl)guanidine (DTG) exhibit high affinity toward both receptor subtypes [15]. Given its very low affinity for the  $\sigma_2$  receptors, (+)-pentazocine is now the “gold standard” molecule used, in its tritiated form, to label  $\sigma_1$  receptors.

In our longstanding research in the field of  $\sigma_1$ R ligands design and discovery, in 2009 we synthesized the series of benzoxazolone derivatives **1** (Figure 1) characterized by high affinity and selectivity towards  $\sigma_1$ receptor subtype [16,17].

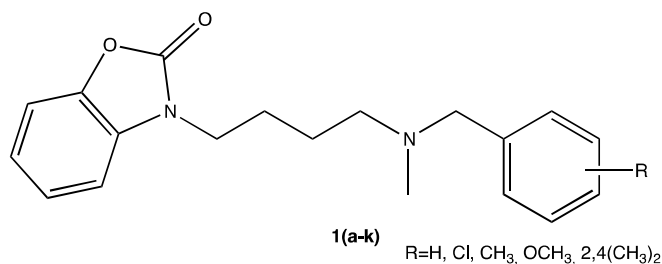


**Figure 1.** Structure of lead compounds **1a-k**

In particular, compounds **1a** (H) and **1d** (4-Cl) showed the most interesting  $\sigma$ 1R affinity within this molecular series, with  $K_i\sigma_1$  values of 2.6 nM and 7.1 nM and selectivity ratio ( $K_i\sigma_2/K_i\sigma_1$ ) of 46.2 and 5.1, respectively. Encouraged by these results, we then selected some of these molecules as training/test set compounds for the construction of a three-dimensional (3D) pharmacophore model for  $\sigma$ 1R binding [17], and the subsequent original development of a  $\sigma$ 1R 3D homology model [18], extensively validated in successive works [19-28]. The information retrieved from the combined application of 3D pharmacophore modeling and molecular dynamics (MD)-based docking and scoring calculations using the 3D  $\sigma$ 1R homology model allowed us to fully characterize the network of intermolecular interactions responsible for the potency of compounds **1** as  $\sigma$ 1R binders.

In the quest of designing, synthesizing, and testing a second generation of effective  $\sigma$ 1R binders, in this work we exploited this wealth of information at hand and explored the effect of the replacement of the benzoxazolone moiety in compounds **1** on  $\sigma$ 1R affinity. Accordingly, based upon modeling design and predictions, a new series of substituted 1-(4-(aryl(methyl)amino)butyl)-heterocyclic derivatives **2-11** (Figure 2) were synthesized and tested for  $\sigma$ 1R binding affinity. Finally, the most promising compounds of this new molecular set were preliminary assessed for their activity profile (agonist/antagonist behavior) in a cell-based assay.

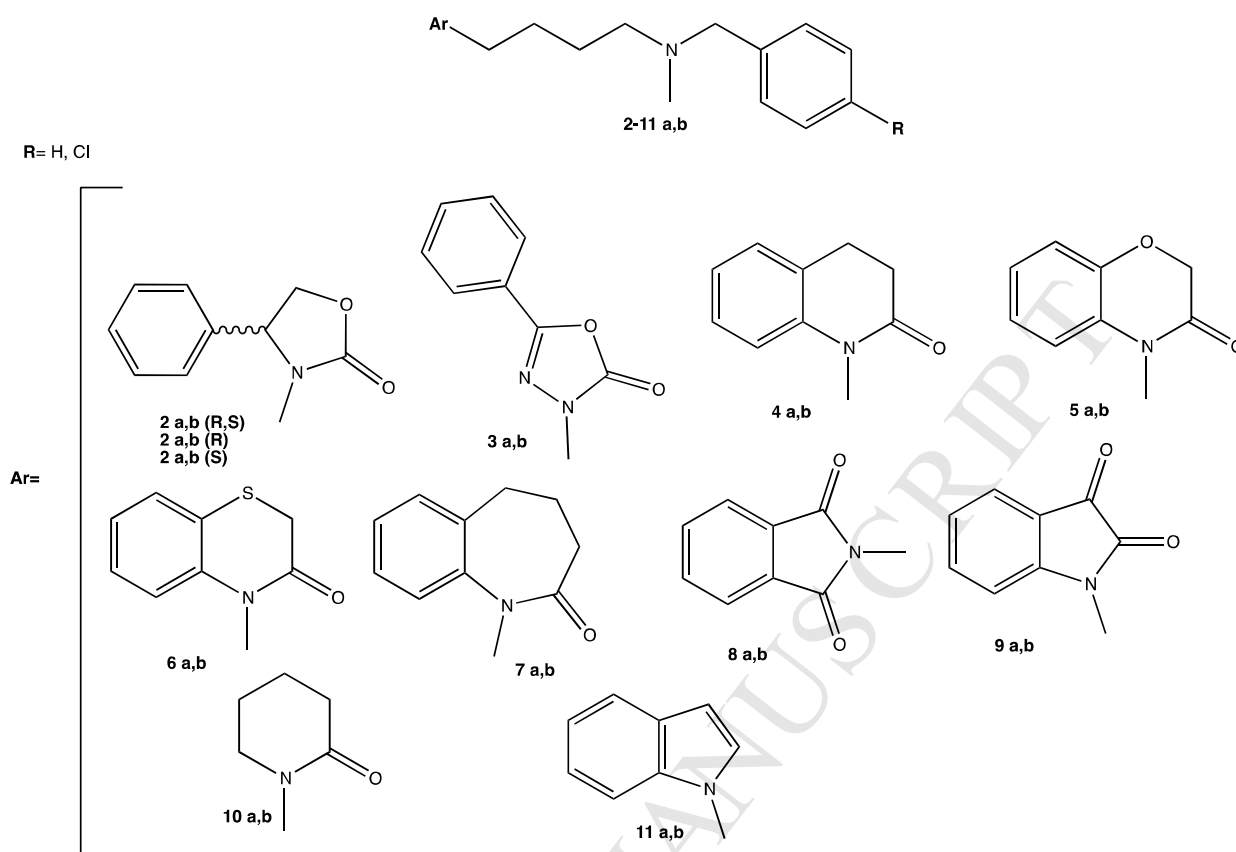


**Figure 2.** Structure of new sigma ligands **2-11a,b**

## 2. Results and discussion

### 2.1 Computer-Aided Design of new 1-(4-(aryl(methyl)amino)butyl)- heterocyclic derivatives

Previous simulations performed on compounds **1a** and **1d** in complex with the 3D homology model of the  $\sigma$ 1R [18,19] led to the identification of a specific map of interaction for each functional group of these molecules, and to the recognition of the protein residues mainly involved in ligand binding. Yet, a detailed quantification of the interaction energies and the derivation of the relevant interaction spectra for these compounds – instrumental to complete the information set required for the design of new derivatives based on **1** - were not carried out at that time. Thus, the optimized structure of the benzoxazolone derivatives **1a** and **1d** were redocked in the binding pocket of the 3D  $\sigma$ 1R model, and the corresponding protein/ligand free energy of binding ( $\Delta G_{\text{bind}}$ ) were calculated via the MM/PBSA (Molecular Mechanics/Poisson-Boltzmann Surface Area) approach [29], yielding values in agreement with the previous report [17], as expected ( $\Delta G_{\text{bind}} = -10.59$  kcal/mol for **1a**, and  $-10.68$  kcal/mol for **1d**, respectively, Table S11). Taking compound **1d** as a proof-of-concept, the analysis of the equilibrated portion

of the respective MD trajectory (Figure 3A) revealed in detail the qualitative pattern of the interactions between this compound and the  $\sigma$ 1R, i.e., the engagement of the basic amine nitrogen of **1d** in a persistent salt bridge with the COO<sup>-</sup> group of D126, and a stable hydrogen bond between the oxygen atom of the benzoxazolone ring of **1d** and the –NH group of the peptidic bond linking residues T151 and V152 of the receptor. Moreover, the MD simulation accounts for the presence of stabilizing  $\pi$ – $\pi$  interactions between the *p*-chlorobenzyl ring of **1d** and the side chains of the protein amino acids W121 and R119 (see also Figure S11 in the supplementary data). Finally, the aromatic fragment of the benzoxazolone moiety and the butyl linker chain of **1d** are nestled in an hydrophobic pocket lined by the side chains of the receptor residues I128, F133, Y173 and L182, with the further stabilizing contribution of E172 (Figure 3A).

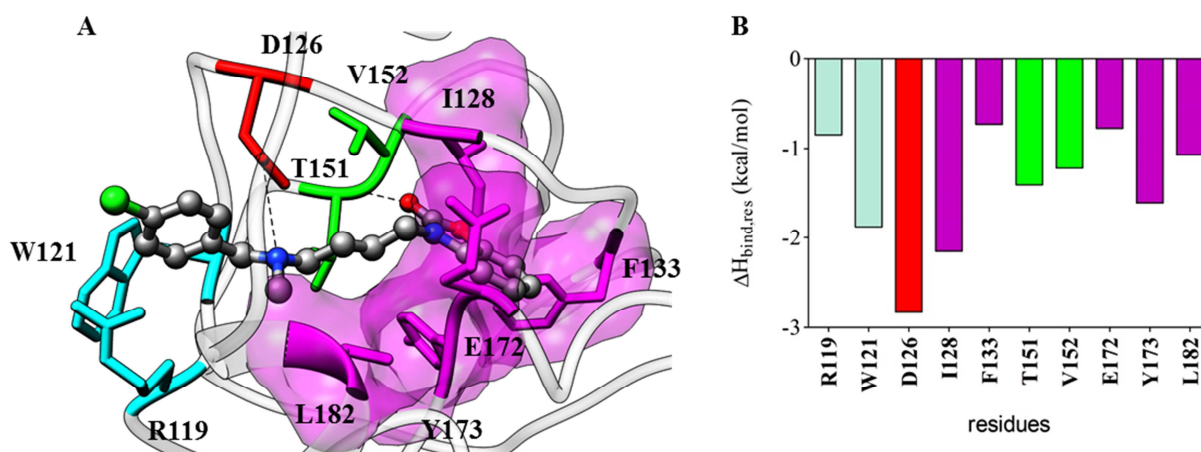


**Figure 3.** (A) Details of compound **1d** in the binding pocket of the  $\sigma$ 1R. Compound **1d** is depicted as atom-colored sticks-and-balls (C, gray, N, blue, O, red, Cl, green). The side chains of  $\sigma$ 1R residues mainly interacting with **1d** are highlighted as colored sticks (R119 and W121, cyan; D126, red; I128, F133, E172, Y173 and L182, magenta; T151 and V152, green) and labeled. The salt bridge and the hydrogen bond are shown as black broken lines. Hydrogen atoms, water molecules, ions, and counterions are omitted for clarity. (B) Per-residue binding free energy decomposition of the selected amino acids for the  $\sigma$ 1R in complex with **1d**.

A quantification of the single contribution of each identified receptor residue to ligand binding was further carried out through a per-residue binding free energy deconvolution (PRBFED) of the enthalpic term ( $\Delta H_{\text{bind, res}}$ ) of the binding free energy, as shown in Figure 3B. The PRBFED analysis confirmed that the network of favorable enthalpic interactions is substantially afforded by the above mentioned  $\sigma$ 1R residues. In particular, the network of hydrophobic interactions involving the alkyl and aromatic fragments of **1d** and the receptor cavity generated by residues I128, F133, E172, Y173 and L182, considerably concurs in stabilizing receptor/ligand binding,

with an overall contribution of -6.34 kcal/mol. Contextually, the  $\pi$  interactions ( $\pi$ -cation and  $\pi$ - $\pi$ , respectively) between the *N-p*-chlorobenzyl ring of **1d** and the side chains of R119 and W121 produce an overall favorable contribution of -2.73 kcal/mol. Noteworthy, the polar interactions afforded by the receptor/ligand permanent salt bridge and hydrogen bond provide a favorable contribution to  $\sigma$ 1R/**1d** binding of -5.46 kcal/mol.

On the basis of these results, we next proceeded with the design of new 1-(4-(aryl(methyl)amino)butyl)- heterocyclic derivatives potentially endowed with comparable, if not enhanced,  $\sigma$ 1R affinity. To the purpose, we reasoned that the *N*-benzyl or the *N-p*-chlorobenzyl amine and the butyl spacer, with their corresponding interactions, were essential for effective  $\sigma$ 1R binding. Thus, we decided to replace the benzoxazolone moiety with others, correlated, heterocyclic scaffolds, in order to explore the conformational space within the relevant binding cavity and to gain further information on the relevance of the specific intermolecular interactions. Accordingly, the following new molecular structures were selected to address specific requirements: (i) the 4-phenyloxazolidin-2-one ((**R**)-**2b** and (**S**)-**2a,b**) and 5-phenyl-1,3,4-oxadiazol-2(3*H*)-one (**3a,b**) derivatives were chosen as non-condensed analogues of the benzoxazolone moiety; (ii) the dihydroquinolin-2(1*H*)-one (**4a,b**), 2*H*-benzo[b][1,4]oxazin-3(4*H*)-one (**5a,b**), 2*H*-benzo[b][1,4]thiazin-3(4*H*)-one (**6a,b**), and 4,5-dihydro-1*H*-benzo[b]azepin-2(3*H*)-one (**7a,b**) substituents were selected to analyze the effect of an increased steric hindrance within the receptor cavity; (iii) the isoindoline-1,3-dione (**8a,b**) and indolin-2,3-dione (**9a,b**) rings were chosen as they are provided with two oxygen atoms, able to potentially perform mutual hydrogen bonds as acceptors with the receptors counterpart; and finally iv) the piperidin-2-one (**10a,b**) and the indole (**11a,b**) scaffolds were selected to study the role of the two peculiar pharmacophore features of the benzoxazolone substituent, i.e., its aromatic part and the hydrogen bond acceptor atom, respectively. In total, a set of 22 new compounds (**2-11**) was designed.

The same docking/MM-PBSA scoring computational procedure described for compounds **1a** and **1d** was next applied to the optimized structures of **2-11** in complex with the  $\sigma$ 1R (Table S1). Figure 4 shows the results of the MM/PBSA analysis, from which a direct structure-affinity correlation can be made.

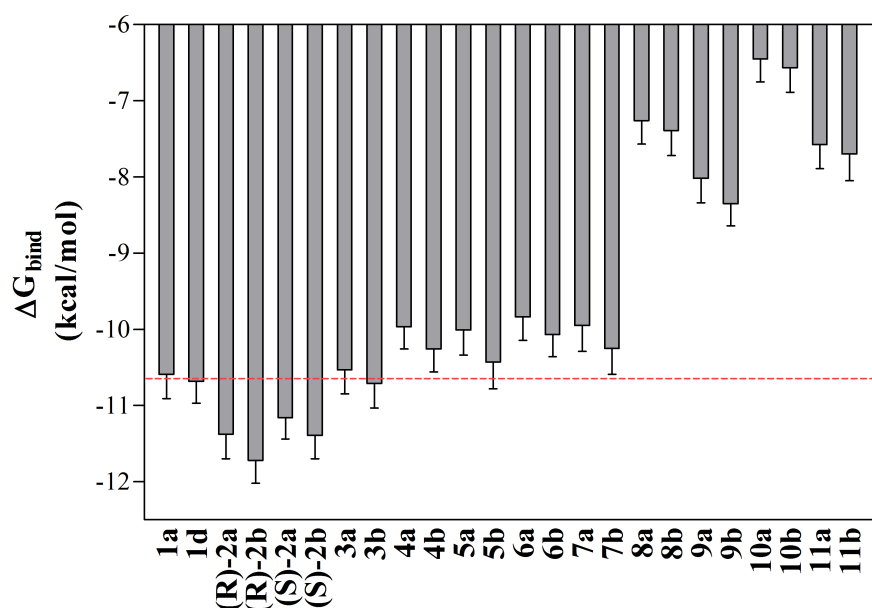


**Figure 4.** *In silico* estimated free energies of binding ( $\Delta G_{\text{bind}}$ ) for the newly designed set of 22  $\sigma 1R$  ligands in complex with receptor. The  $\Delta G_{\text{bind}}$  of the benzoxazolone derivatives **1a** and **1d** are also shown for comparison, the dotted red line serving as a guide.

As seen in Figure 4, computational data predict that the replacement of the benzoxazolone moiety with a non-constrained analogous such as the 4-phenyloxazolidin-2-one group in derivatives **(R)-2a,b** and **(S)-2a,b** could slightly increase the affinity of these compounds for the receptor, derivative **(R)-2b** exhibiting the best  $\Delta G_{\text{bind}}$  value of -11.72 kcal/mol. Furthermore, in agreement with previous observations [21,23,28], simulations indicate that the eventual presence of a stereo center does not substantially affect the interactions of the relevant compound with the receptor, since all the phenyloxazolidinones are provided with comparable  $\sigma 1R$  affinity (Figures 4 and 5, Table S11). Application of the PRBFED analysis further confirmed the interpretation of the overall free energy of binding values: all  $\sigma 1R$  residues involved in ligand binding establish the same qualitative interactions with the ligands, and afford a favorable  $\Delta H_{\text{bind, res}}$  contribution comparable with those detected with lead compounds **1a** and **1d** (Figure 5B).

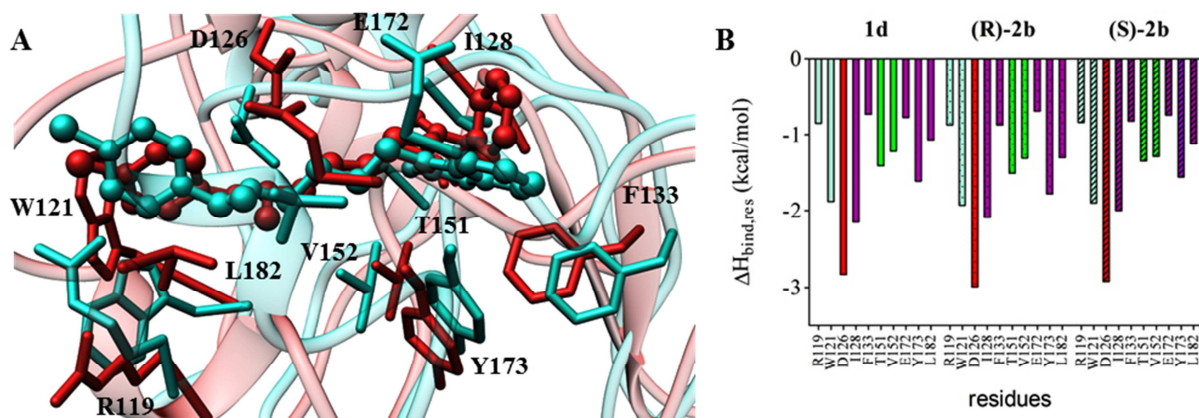


**Figure 5.** (A) Superposition of equilibrated MD snapshots of the  $\sigma$ 1R in complex with **1d** (light sea green) and **(R)-2b** (firebrick). Hydrogen atoms, water molecules, ions, and counterions are omitted for clarity. (B) Comparison of the per-residue binding enthalpy decomposition  $\Delta H_{\text{bind, res}}$  for compounds **1d**, **(R)-2b** and **(S)-2b** in complex with the  $\sigma$ 1R.

On the other hand, the  $\Delta G_{\text{bind}}$  values predicted for compounds **4-7** point to a small decrease of  $\sigma$ 1R binding capability for these molecules compared to the benzoxazolone derivatives **1a** and **1d**, with free energy of binding values in the range -9.84 – -10.43 kcal/mol (Figure 4, Table S11). In fact, the presence of the amidic group in each scaffold allow them to perform the fundamental hydrogen bond with the receptor via their acceptor oxygen, while the aromatic fragment of the corresponding heterocyclic moiety can exploit stabilizing interactions while nicely encased within the  $\sigma$ 1R hydrophobic cavity.

The results obtained with the remaining derivatives **8-11** deserved a more specific interpretation. From a computational perspective, the lack of one of the important pharmacophore requirements in the piperidin-2-one (**10a,b**) and the indole (**11a,b**) derivatives leads to a plummet in the corresponding affinity for the  $\sigma$ 1R, with a loss in  $\Delta G_{\text{bind}}$  of about 4 and 3 kcal/mol, respectively. The absence of the aromatic fragment in the piperidinone derivatives **10a,b** not only affects the hydrophobic interactions with the  $\sigma$ 1R residues I128, F133, E172, Y173, and L182, but also, via a sort of domino effect, negatively reflects on the bound ligand conformation, with a consequent drastic reduction of the entire interaction spectrum, as testified in Figure 6. The same behavior is reproduced by the indole derivatives **11a,b**, for which not only the contributions of T151 and V152 are zero, as expected, but also the rest of the  $\sigma$ 1R residues involved in ligand binding diminish their favorable contribution to binding enthalpy.

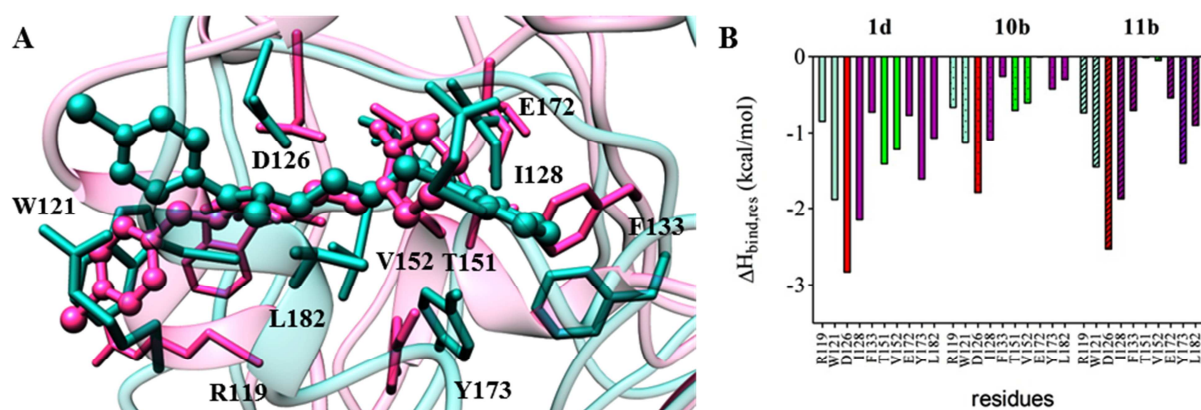


**Figure 6.** (A) Superposition of equilibrated MD snapshots of the  $\sigma$ 1R in complex with **1d** (light sea green) and **10b** (hot pink). Hydrogen atoms, water molecules, ions and counterions are omitted for clarity. (B) Comparison of the per residue binding enthalpy decomposition  $\Delta H_{\text{bind, res}}$  for compounds **1d**, **10b** and **11b** in complex with  $\sigma$ 1R.

More interesting are the computational results obtained with isoindoline-1,3-dione (**8a,b**) and indolin-2,3-dione (**9a,b**) derivatives. Although the structures of these compounds are provided with all optimal pharmacophore requirements for  $\sigma$ 1R binding, the insertion of a further hydrogen acceptor group in the heterocyclic scaffold substantially seems to compromise the affinity of these molecules for the  $\sigma$ 1R. In fact, as the inspection of the relevant MD trajectory reveals, to maintain the interaction with the  $-\text{NH}$  group of the backbone between T151 and V152 both the hetero-aromatic groups pay the cost of a configuration rearrangement within the binding cavity; this, in turn, impairs the rest of the favorable interactions with the other  $\sigma$ 1R residues involved in binding, as shown in Figure 7. The resulting binding conformations assumed by compounds **8a,b** and **9a,b** do not allow them to satisfactorily snug their aromatic fragment within the receptor binding cavity, the consequent reorganization of the N,N-arylmethyl amine moiety preventing this group from exploiting optimal interactions with residues R119, W121, and D126.

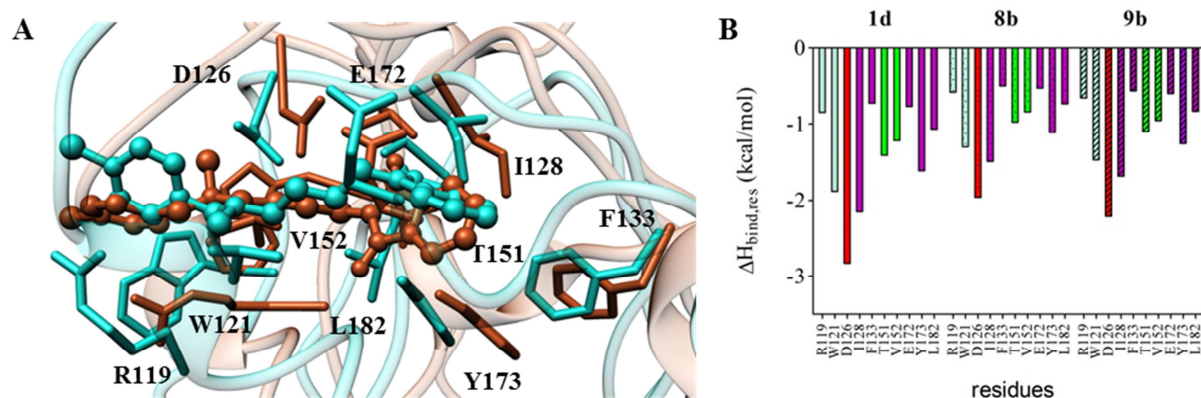
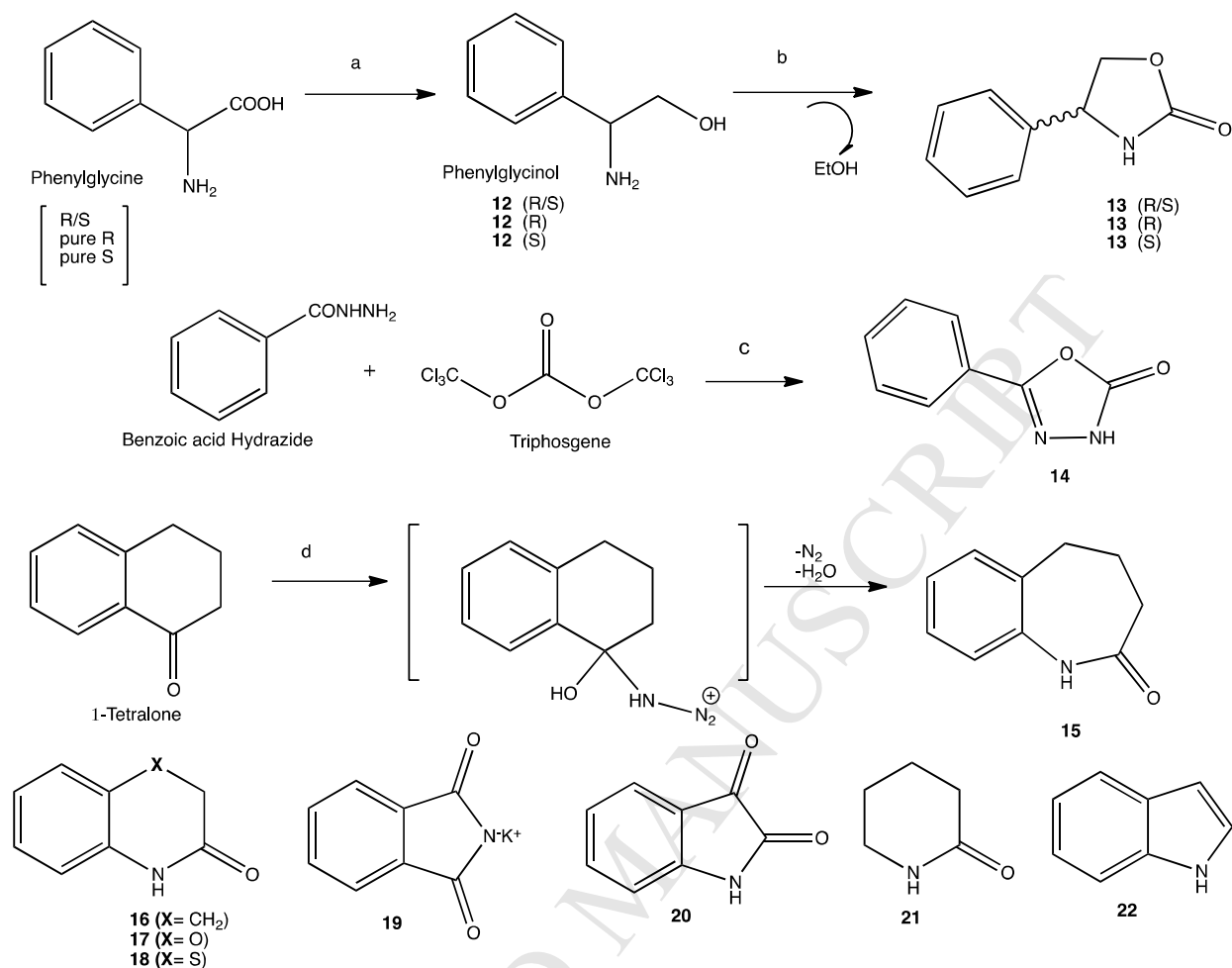


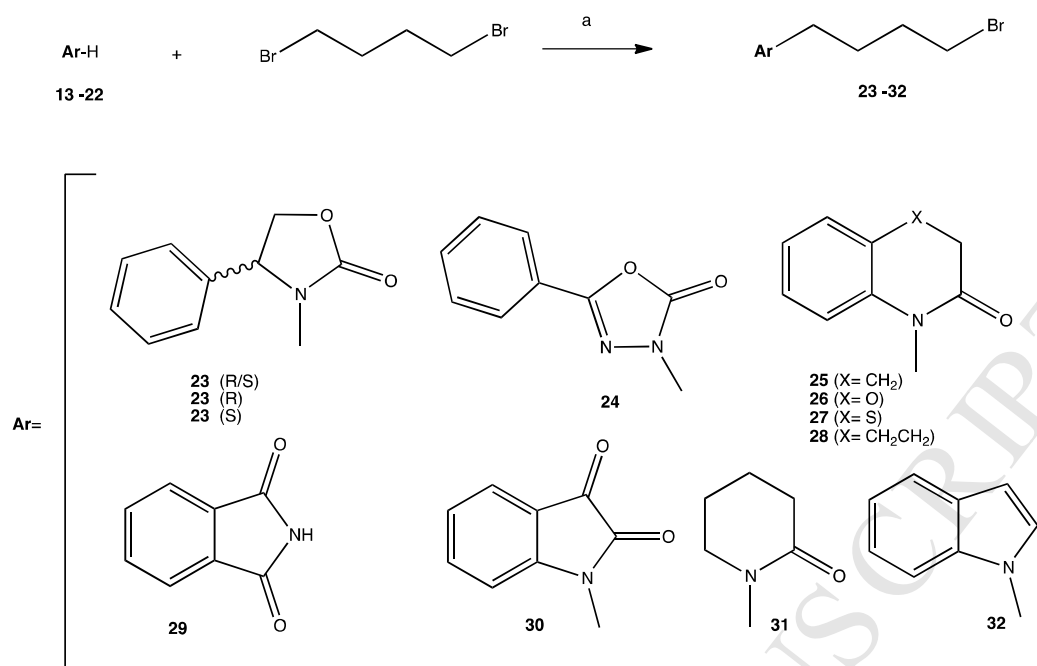
**Figure 7.** (A) Superposition of equilibrated MD snapshots of the  $\sigma$ 1R in complex with **1d** (light sea green) and **8b** (sienna). Hydrogen atoms, water molecules, ions and counterions are omitted for clarity. (B) Comparison of the per-residue binding enthalpy decomposition  $\Delta H_{\text{bind, res}}$  for compounds **1d**, **8b**, and **9b** in complex with  $\sigma$ 1R.

## 2.2 Chemistry

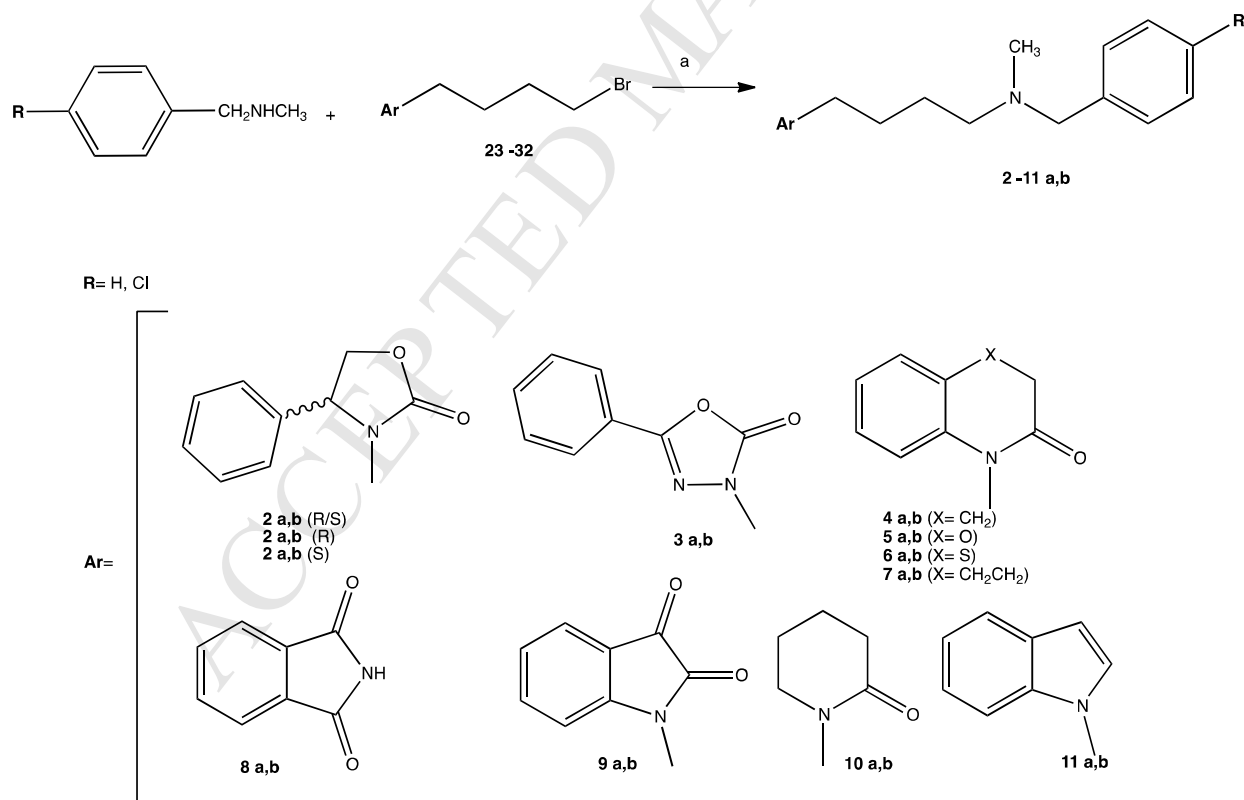
All derivatives **2-11** were synthesized starting from the corresponding intermediate (Schemes 1 and 2), according to the synthetic pathway reported in Scheme 3 (Table SI2). The synthetic pathway of each derivative started from the relevant commercially available scaffolds: 3,4-dihydroquinolin-2(1*H*)-one (**16**), 2*H*-benzo[*b*][1,4]-oxazin-3(4*H*)-one (**17**), 2*H*-benzo[*b*][1,4]-thiazin-3(4*H*)-one (**18**), potassium phthalimide (**19**), indolin-2,3-dione (**20**), piperidin-2-one (**21**) and indole (**22**), respectively. The series **2a,b** was obtained as racemate form (**2a,b**), as well as enantiomerically pure R (**R-2a,b**) and S (**S-2a,b**) isomers, starting from pure phenylglycine (R/S, R and S). Compounds **3a,b** were obtained from the intermediate 5-phenyl-1,3,4-oxadiazol-2(3*H*)-one **14** resulting from cyclization of benzoic acid hydrazide with triphosgene. Series **7a,b** was obtained following Schmidt cyclization starting from 1-tetralone and sodium azide in conc.  $\text{H}_2\text{SO}_4$ . The *N*-methyl-1-phenylmethanamine is commercially available, while the 1-(4-chlorophenyl)-*N*-methylmethanamine was obtained by reaction from 4-chlorobenzyl chloride and methylamine solution.



**Scheme 1.** Synthesis of intermediate **12-22** (phenylglycine, benzoic acid hydrazide, triphosgene, 1-tetralone and compounds **16-22** are commercially available). Reagents and conditions: a) NaBH<sub>4</sub>, I<sub>2</sub>, THF/100°C, MeOH, rt then KOH 20% 4h; b) (EtO)<sub>2</sub>CO 130°C; c) H<sub>2</sub>O/Tol. 0°C; d) H<sub>2</sub>SO<sub>4</sub> conc., NaN<sub>3</sub>, Toluene 0°C 0.5h, rt overnight.



**Scheme 2.** Synthesis of intermediate **23-32**. Reagents and conditions: a) K<sub>2</sub>CO<sub>3</sub>/KI (cat.), ACN, 100°C, 6-12h.



**Scheme 3.** Synthesis of final compounds **2-11a,b**. Reagents and conditions: a) K<sub>2</sub>CO<sub>3</sub>, ACN, 100°C, 6-12h.

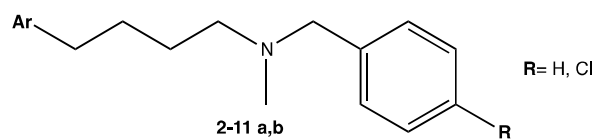
### 2.3 Receptor binding studies

$\sigma$ 1R and  $\sigma$ 2R affinities of the test compounds were determined in competition experiments by radiometric assays, using [ $^3$ H]-(+)-Pentazocine as radioligand for the  $\sigma$ 1R assay, and [ $^3$ H]-DTG as radioligand in the  $\sigma$ 2R assay. Compounds **2-11a,b** were tested against  $\sigma$ 1R and  $\sigma$ 2R of animal origin prepared from guinea pig brain and rat liver, respectively.

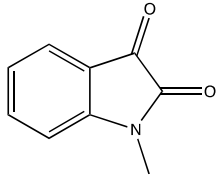
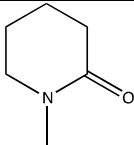
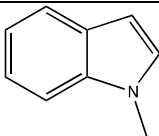
In principle, the receptor binding studies on  $\sigma$ 1R confirmed the structure-affinity relationship predicted by the computational approach, as testified from the strict correlation between the calculated free energies of binding and the corresponding  $K_i\sigma$ 1 values listed in Table 1 ( $R^2=0.84$ ). In fact, in agreement with MM-PBSA calculations, the 4-phenyloxazolidin-2-one derivatives (**2a,b**, (**R**)-**2a,b** and (**S**)-**2a,b**), and the 5-phenyl-1,3,4-oxadiazol-2(3H)-one (**3a,b**) compounds are experimentally ranked as the best  $\sigma$ 1R binders, with a  $K_i\sigma$ 1 values in the range 0.95-25 nM. Also, these compounds are provided with a good selectivity against the  $\sigma$ 2R subtype, for which they show affinity values at least one order of magnitude lower with respect to the  $\sigma$ 1R counterpart. The slight decrease in  $\sigma$ 1R affinity predicted by modeling for compounds **4-7** as a consequence of the replacement of the benzoxazolone moiety with a larger heterocyclic group is confirmed by the corresponding experimental data (Table 1). Interestingly, however, these molecules preserve a good selectivity profile against the  $\sigma$ 2 subtype.

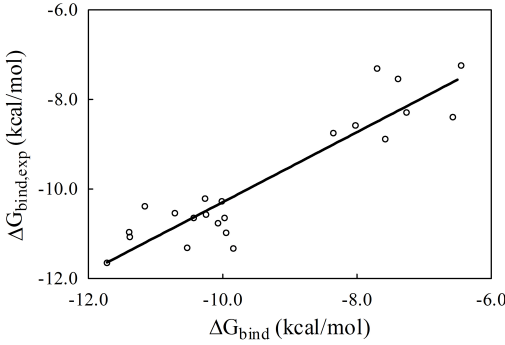
The experimental analysis carried out for the remaining new derivatives **8-11** confirmed that the absence of the fundamental heterocyclic groups dramatically affects receptor/ligand binding, the corresponding  $K_i\sigma$ 1 spanning the high nanomolar - micromolar concentration range.

It is interesting to note that, although the tested  $K_i\sigma$ 2 were very weak, all compounds show a similar behavior against the  $\sigma$ 2R subtype, with affinity values all of the order of hundreds of nanomolar. The  $\sigma$ 2 receptor is even more enigmatic than  $\sigma$ 1R, and the information about its binding site for the ligands is exceedingly scarce and fragmented; therefore any computational structure-affinity relationship derivation can be barely attempted, if at all. Anyway, on the basis of these results, we are be tempted to speculate that the  $\sigma$ 2R region in which the heterocyclic scaffold is likely to be nestled might be characterized by higher adaptability with respect to  $\sigma$ 1R, thereby accommodating the presence of different chemical moieties without requiring major energetical penalties. If verified, this information could be exploited in the future studies to investigate and rationalize the molecular determinants for the  $\sigma$ 2R binding.



Cpd	Ar	R	$K_i\sigma_1$ (nM)	$K_i\sigma_2$ (nM)	$K_i\sigma_2/K_i\sigma_1$
<b>2a</b>		H	2.7±0.9	89±19	32
<b>2b</b>		Cl	0.95±0.13	93±17	98
<b>(R)-2a</b>		H	7.7±0.7	>3000	>390
<b>(R)-2b</b>		Cl	2.9±0.6	603	208
<b>(S)-2a</b>		H	25±5	190	7.6
<b>(S)-2b</b>		Cl	9.3±0.8	317	8.1
<b>3a</b>		H	5.2±1.9	110	17
<b>3b</b>		Cl	18.7±1.3	315	16.8
<b>4a</b>		H	16±6	222	13.9
<b>4b</b>		Cl	33±9	239	7.2
<b>5a</b>		H	30±8	274	9.1
<b>5b</b>		Cl	16±3	119	7.4
<b>6a</b>		H	5.0±1	105	21
<b>6b</b>		Cl	13±3	169	13
<b>7a</b>		H	9.0±3	254	28
<b>7b</b>		Cl	18±2	412	23
<b>8a</b>		H	844	621	0.73
<b>8b</b>		Cl	>3000	42±24	<0.014

<b>9a</b>		H	519	237	0.46
<b>9b</b>		Cl	385	173	0.45
<b>10a</b>		H	>3000	>3000	n.d.
<b>10b</b>		Cl	770	252	0.33
<b>11a</b>		H	310	252	0.81
<b>11b</b>		Cl	4400	1200	0.27
<b>Haloperidol</b>	-	-	6.6±0.9	78±2.0	11.8
<b>DTG</b>	-	-	71±8	54±8	0.8

**Table 1.**  $\sigma$ 1R and  $\sigma$ 2R affinities of the synthesized compounds **2-11a,b**. All compounds with highest affinities (<100 nM) were tested in triplicates. n.d.: not determined. The last row shows the correlation ( $R^2=0.84$ ) between the predicted values  $\Delta G_{\text{bind}}$  and the corresponding experimental  $\Delta G_{\text{bind,exp}}$ , calculated using the following relationship:  $\Delta G_{\text{bind,exp}} = -RT \ln(1/K_i\sigma_1)$ .

#### 2.4 Functional characterization

With the aim of performing an investigation of the cytotoxic activity of this new series of  $\sigma$ 1R ligands, and attempting a preliminary functional characterization of their eventual agonist/antagonist profile, we compared the toxic effects of a set of novel compounds obtained on the SH-SY5Y neuroblastoma cell line with those measured for NE-100 and haloperidol (two commonly accepted  $\sigma$ 1R antagonist) and pentazocine (the gold standard  $\sigma$ 1R agonist) (Figure 8). Although SH-SY5Y cells seem to express  $\sigma$ 1R at moderate level [30], previous works used this human cell line of neuronal origin for  $\sigma$ 1R studies [31-33] and obtained results overlapping with those obtained with guinea pig brain subcellular fraction [34].

To the purpose, we followed the approach originally proposed by Zeng et al. for  $\sigma$ 2R ligands [35], based on the MTT assay. The underlying assumption for performing these tests is that  $\sigma$ 1R

agonists should promote cytoprotection via target activation, while antagonists should be generally endowed with an opposite (i.e., cytotoxic) effect [36]. Specifically, we tested those new compounds characterized by the highest  $\sigma$ 1R affinity (that is, **2b (R)-2b**, **(S)-2b**, **3a**, and **6a**), while the lead compounds **1a** and **1d** were also tested for comparison.

Accordingly to its recognized antagonist profile, NE-100 has a potent cytotoxic effect, as clearly shown in Figure 9, where the effect exerted by the best  $\sigma$ 1R binders is also shown as % of NE-100 cytotoxicity at 50  $\mu$ M (100%).

Considering the criteria adopted, the behavior of pentazocine and haloperidol in SH-SY5Y cells is consistent with an activity of agonist and antagonist compounds, respectively. Actually, haloperidol showed a cytotoxic effect (99%) at 50  $\mu$ M strictly comparable with NE-100, while pentazocine exhibited a negligible cytotoxicity (4.4%) at the same concentration. The benzoxazolone derivatives **1a** and **1d** displayed an ambiguous cytotoxicity profile, since their corresponding values are comprised between 50% and 75%. Clearly, further investigations are required in this respect. On the other hand, the newly designed derivatives **2b (R)-2b**, **(S)-2b**, **3a**, and **6a** all exhibit a plausible  $\sigma$ 1R agonist profile, seemingly in line with the low cytotoxic activity detected for pentazocine. In particular, the 4-phenyloxazolidin-2-one derivatives, both as pure enantiomers **(R)-2b**, **(S)-2b** and in their racemic form **2b**, demonstrate very low cytotoxic effects (< 15%), strictly comparable to the prototypical  $\sigma$ 1R agonist, as inferred from Figure 9. For the record, these compounds are also characterized by the best  $\sigma$ 1R affinity along the new series of  $\sigma$ 1R designed and tested in the present work (Table 1).

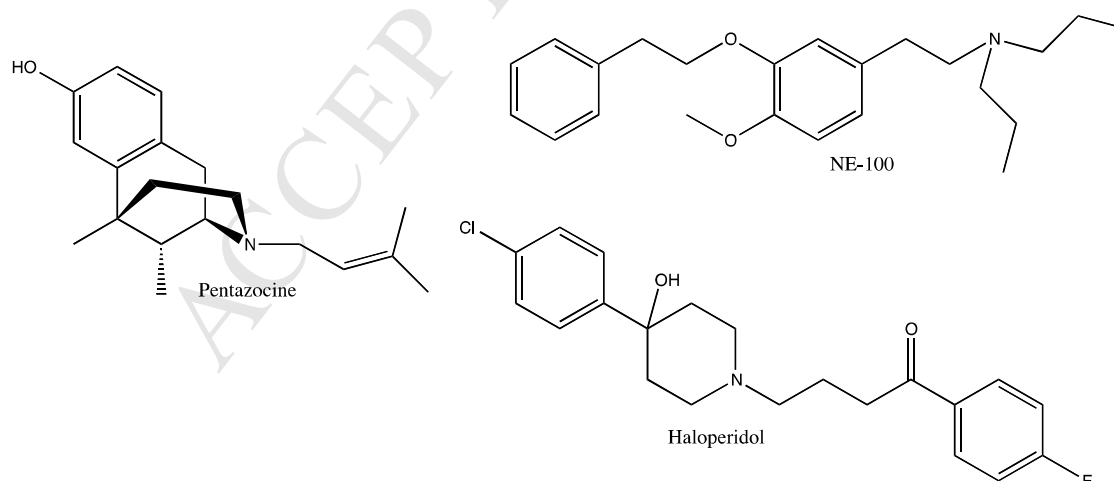


**Figure 8.** Test compounds used for functional assay to define  $\sigma$ 1R agonist/antagonist profile:

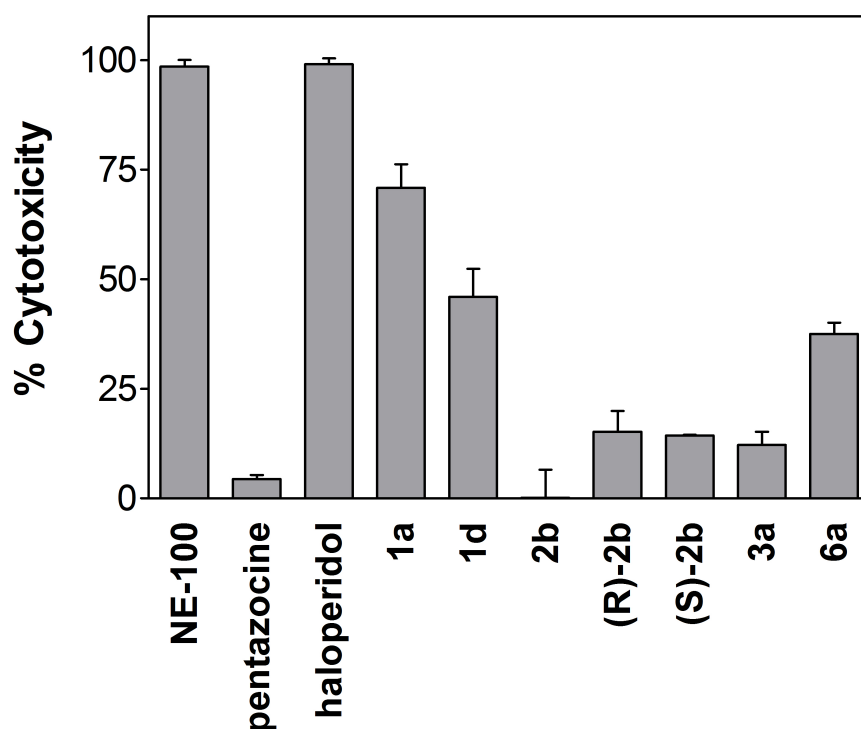


**Figure 9.** Cytotoxicity of  $\sigma_1$ R ligands as obtained from the MTT assay. SH-SY5Y cells were treated with different  $\sigma_1$ R ligands (50  $\mu$ M) for 48h. MTT assay was then performed, cytotoxicity of compounds was determined, and data were reported as % of NE-100 cytotoxicity at 50  $\mu$ M (100%). The bars represent the mean  $\pm$  SD from three independent experiments performed in triplicate.

### 3. Conclusions

On the basis of the molecular information retrieved by the *in silico* analysis of the binding mode of the two lead benzoxazolone derivatives **1a** and **1d**, both endowed with high  $\sigma_1$ R affinity ( $K_i\sigma_1 = 2.6$  and  $7.1$  nM, respectively), we designed and synthesized the new series of derivatives **2-11a,b**, with a twofold aim of (i) dissecting the effect of the replacement of the benzoxazolone moiety on sigma 1 receptor affinity, and (ii) preliminarily evaluating the behavior of these compounds as  $\sigma_1$ R agonists or antagonists. All new molecules maintain the 1-(4-(aryl(methyl)amino)butyl)- spacer characterizing the compound series **1**, whereas the benzoxazolone moiety, linked to the butyl chain, has been replaced with others, correlated, heterocyclic scaffolds to obtain the corresponding 4-phenyloxazolidin-2-one (**2a,b**, **(R)-2a,b** and **(S)2a,b**), 5-phenyl-1,3,4-oxadiazol-2(3*H*)-one (**3a,b**), dihydroquinolin-2(1*H*)-one (**4a,b**), 2*H*-benzo[b][1,4]oxazin-3(4*H*)-one (**5a,b**), 2*H*-benzo[b][1,4]thiazin-3(4*H*)-one (**6a,b**) and 4,5-

dihydro-1*H*-benzo[*b*]azepin-2(3*H*)-one (**7a,b**), isoindoline-1,3-dione (**8a,b**), indolin-2,3-dione (**9a,b**), piperidin-2-one (**10a,b**) and indole (**11a,b**) derivatives.

The results achieved by scoring the affinity of these molecules for the  $\sigma$ 1R via their molecular dynamics simulations in complex with our 3D  $\sigma$ 1R model allowed us to predict that, from the perspective of receptor binding ability, modifications of the benzoxazolone moiety are well tolerated only if the new molecular scaffolds preserve the peculiar molecular determinants for the optimal encasement in the relevant  $\sigma$ 1R binding cavity. In fact, the new derivatives **2-7**, in which the aromatic substituent and the hydrogen bond acceptor atom are preserved, display a binding capacity comparable to, or even slightly higher (as in the case of the derivatives 4-phenyloxazolidin-2-one **2a,b**) to that of the lead compounds **1a** and **1d**. Conversely, when one of the pharmacophore requirements is missing (as in the piperidone (**10a,b**) or in the indole (**11a,b**) derivatives), the favorable interactions established between the  $\sigma$ 1R and the ligand significantly decreases, with effects extending, in a domino effect, beyond the receptor hydrophobic cavity directly involved in ligand binding. Finally, it is interesting to highlight that the addition of a supplementary element, i.e. an additional hydrogen bond acceptor (e.g., isoindolindiones **8a,b** and indolindiones **9a,b**), leads to a substantial impairment of the resulting compound  $\sigma$ 1R binding capability, by virtue of a suboptimal conformation of the aromatic fragment nestled in the receptor binding cavity.

All computer-based predictions were substantiated by the experimental characterization of the  $\sigma$ 1R affinity of all new compounds through radioligand binding assays of the  $K_i$  values against both sigma receptor subtypes. The analysis confirmed the quality of the *in silico* prediction with an outstanding agreement between the calculated  $\sigma$ 1R affinity and the experimental inhibitory concentrations. Moreover, the experiments revealed a clear preference of the new derivative **2-7** for the  $\sigma$ 1R with a good selectivity profile against the  $\sigma$ 2 receptor subtypes.

Finally, the MTT viability assay on human neuroblastoma cells (SH-SY5Y) was performed in order to test the cytotoxic effects of the novel compounds. These data were also useful for a preliminary evaluation of the agonist/antagonist behavior on a selection of the best  $\sigma$ 1R binder in the new series. According to these tests, the new 4-phenyloxazolidin-2-one derivatives **2b**, (**R**)-**2b** and (**S**)-**2b** demonstrated a very low level of cytotoxicity, comparable with that obtained with the  $\sigma$ 1R prototypical agonist pentazocine. This property, coupled with their remarkable  $\sigma$ 1R affinities ( $K_i$  values in the low nanomolar range), outlines these compounds as the most

promising candidates of the series to exploit them as new pharmacologic agents for further and more specific investigation on the  $\sigma$ 1R biologic activity.

## 4. Experimental

### 4.1 Computational details

The optimized structure of all compounds was docked into the putative binding pockets for the sigma1 receptor by applying a consolidated procedure [18-28] with AutoDock 4.2 [37]. For each compound, only the molecular conformation satisfying the combined criteria of having the lowest (i.e., more favorable) Autodock energy and belonging to a highly populated cluster was selected to carry out for further modeling. The ligand/receptor complexes obtained from the docking procedure was further refined in Amber 14 [38] using the quenched molecular dynamics (QMD) method as previously described [18-28]. According to QMD, the best energy configuration of each complex resulting from this step was subsequently solvated by a cubic box of TIP3P [39] water molecules extending at least 10 Å in each direction from the solute. The system was neutralized and the solution ionic strength was adjusted to the physiological value of 0.15 M by adding the required amounts of Na<sup>+</sup> and Cl<sup>-</sup> ions. Each solvated system was relaxed by 500 steps of steepest descent followed by 500 other conjugate-gradient minimization steps and then gradually heated to a target temperature of 300 K in intervals of 50 ps of NVT MD, using a Verlet integration time step of 1.0 fs. The Langevin thermostat was used to control temperature, with a collision frequency of 2.0 ps<sup>-1</sup>. The protein was restrained with a force constant of 2.0 kcal/(mol Å), and all simulations were carried out with periodic boundary conditions. Subsequently, the density of the system was equilibrated via MD runs in the isothermal-isobaric (NPT) ensemble, with isotropic position scaling and a pressure relaxation time of 1.0 ps, for 50 ps with a time step of 1 fs. All restraints on the protein atoms were then removed, and each system was further equilibrated using NPT MD runs at 300 K, with a pressure relaxation time of 2.0 ps. Three equilibration steps were performed, each 2 ns long and with a time step of 2.0 fs. To check the system stability, the fluctuations of the rmsd of the simulated position of the backbone atoms of the receptor with respect to those of the initial protein were monitored. All chemophysical parameters and rmsd values showed very low fluctuations at the end of the equilibration process, indicating that the systems reached a true equilibrium condition. The equilibration phase was

followed by a data production run consisting of 40 ns of MD simulations in the canonical (NVT) ensemble. Only the last 20 ns of each equilibrated MD trajectory were considered for statistical data collections. A total of 1000 trajectory snapshots were analyzed the each ligand/receptor complex. The binding free energy,  $\Delta G_{\text{bind}}$ , between the ligands and the signal receptor was estimated by resorting to the MM/PBSA approach implemented in Amber 14. According to this well validated methodology [18-28], the free energy was calculated for each molecular species (complex, receptor, and ligand), and the binding free energy was computed as the difference:

$$\Delta G_{\text{bind}} = G_{\text{complex}} - (G_{\text{receptor}} + G_{\text{ligand}}) = \Delta E_{\text{MM}} + \Delta G_{\text{sol}} - T\Delta S$$

in which  $\Delta E_{\text{MM}}$  represents the molecular mechanics energy,  $\Delta G_{\text{sol}}$  includes the solvation free energy and  $T\Delta S$  is the conformational entropy upon ligand binding. The per residue binding free energy decomposition was performed exploiting the MD trajectory of each given compound/complex, with the aim of identifying the key residues involved in the ligand/receptor interaction. This analysis was carried out using the MM/GBSA approach [40], and was based on the same snapshots used in the binding free energy calculation. All simulations were carried out using the Pmemd modules of Amber 14, running on our *Mose25* CPU/GPU calculation cluster.

#### 4.2 Chemistry

Commercially available chemicals were of reagents grade and used as received. Column chromatography was performed on Silica Gel 60 (230-400 mesh, Merk) and reaction courses and product mixtures were routinely monitored by thin-layer chromatography (TLC) on silica gel precoated F<sub>254</sub> Merck plates. Melting points were determined with a Büchi 510 capillary apparatus or a Stuart SMP300, and are uncorrected. Infrared spectra were recorded on a Perkin Elmer RXI spectrophotometer in nujol mulls. Proton nuclear magnetic resonance (<sup>1</sup>H-NMR) spectra were determined on a Varian Gemini 200 MHz, a Jeol 400 MHz and a Varian Inova 500 MHz; chemical shifts are reported as  $\delta$  (ppm) in CDCl<sub>3</sub> solution (0.05% v/v TMS). ESI-MS spectra were obtained on a Bruker Daltonics Esquire 4000 spectrometer by infusion of a solution of the sample in MeOH.

#### 4.2.1 Synthesis of (R,S)-4-phenyloxazolidin-2-one **13** [41,42]

To a solution of 2.5 g (66.0 mmol) of NaBH<sub>4</sub> in 125 ml of THF at 0°C, 8.4 g of I<sub>2</sub> (33.0 mmol) dissolved in the minimum amount of THF, were slowly added. When the solution turns white, 5.0 g of (R,S)-phenylglycine were added. The mixture was heated under reflux for 18h under TLC monitoring (CH<sub>2</sub>Cl<sub>2</sub>/EtOH 9:1). The solution was allowed to cool then added of 4 ml of MeOH until it turns clear. The solvents were removed under reduced pressure.

The solid residue has been taken with 60 ml of a KOH 20% acq. solution and allowed to stir for 4h at room temperature. CH<sub>2</sub>Cl<sub>2</sub> was added and the organic phase was separated, washed with water, dried with Na<sub>2</sub>SO<sub>4</sub> and concentrated in vacuum to afford 4.3g (95%) of (R,S)-phenylglycinol **12** as a light-yellow oil.

<sup>1</sup>H NMR (CDCl<sub>3</sub>-TMS) ppm (δ): 2.84 (broad s., 3H, NH<sub>2</sub> + OH); 3.46 (m, 1H<sub>a</sub>, CH<sub>2</sub>); 3.56 (m, 1H<sub>b</sub>, CH<sub>2</sub>); 3.87 (m, 1H, CH); 7.20 (m, 5H, arom.). MS: m/z 138 [MH<sup>+</sup>].

In the same manner pure (R)-phenylglycinol (**R**)-**12** and pure (S)-phenylglycinol (**S**)-**12** were obtained, starting from the corresponding R- and S-phenylglycine.

A dry 250 ml three-necked round bottom flask equipped with a thermometer and a 10 cm vigreux column with a distillation head, was charged with 4.3 g of the (R,S)-phenylglycinol (31.4 mmol) obtained and added of 9.3 g of diethyl carbonate (79.0 mmol) and 0.43 g of K<sub>2</sub>CO<sub>3</sub> (3.10 mmol). The mixture was heated carefully to 130-140°C and the ethanol was distils as it formed. The oily residue was cooled and added by 50 ml of CH<sub>2</sub>Cl<sub>2</sub> to facilitate the filtration of the remaining potassium carbonate. The organic phase was then washed with a saturated solution of NaHCO<sub>3</sub>, separated and dried over anhydrous Na<sub>2</sub>SO<sub>4</sub>, filtrate and evaporated *in vacuo*. The residue was crystallized from AcOEt/Etp (1:3) to afford 4.3 g (26.4 mmol, 85%) of **13** as a white solid; mp 134-136°C.

<sup>1</sup>H-NMR (CDCl<sub>3</sub>/TMS) δ: 4.22 (dd 1H, CH<sub>2</sub> oxad., J=8.6; 7.0 Hz); 4.77 (dd, 1H, CH oxad., J=8.6; 8.6 Hz); 4.98 (dd, 1H, CH<sub>2</sub> oxad., J= 8.6; 7.0 Hz); 5.40 (broad s., 1H, NH oxad. disappearing on D<sub>2</sub>O); 7.40 (m, 5H, arom.). MS: m/z 164 [MH<sup>+</sup>].

In an analogous way the pure isomers (R)-4-phenyloxazolidin-2-one (**R**)-**13** and (S)-4-phenyloxazolidin-2-one (**S**)-**13** were obtained:

#### 4.2.2. (R)-4-phenyloxazolidin-2-one (**R**)-**13**

White solid; m.p.: 126-128°C; Yield (%): 85. <sup>1</sup>H-NMR (CDCl<sub>3</sub>/TMS) δ: 4.22 (dd 1H, CH<sub>2</sub> oxad., *J*= 8.6; 7.0 Hz); 4.77 (dd, 1H, CH oxad., *J*= 8.6; 8.6 Hz); 4.98 (dd, 1H, CH<sub>2</sub> oxad., *J*= 8.6; 7.0 Hz); 5.40 (broad s., 1H, NH oxad. disappearing on D<sub>2</sub>O); 7.40 (m, 5H, arom.). MS: m/z 164 [MH<sup>+</sup>].

#### 4.2.3. (S)-4-phenyloxazolidin-2-one (**S**)-**13**

White solid; m.p.: 124-126°C; Yield (%): 77. <sup>1</sup>H-NMR (CDCl<sub>3</sub>/TMS) δ: 4.22 (dd 1H, CH<sub>2</sub> oxad., *J*= 8.6; 7.0 Hz); 4.77 (dd, 1H, CH oxad., *J*= 8.6; 8.6 Hz); 4.98 (dd, 1H, CH<sub>2</sub> oxad., *J*= 8.6; 7.0 Hz); 5.40 (broad s., 1H, NH oxad. disappearing on D<sub>2</sub>O); 7.40 (m, 5H, arom.). MS: m/z 164 [MH<sup>+</sup>].

#### 4.2.4. 5-Phenyl-1,3,4-oxadiazol-2(3H)-one **14** [43]

To an ice-bath solution of benzoic acid hydrazide (2.5 g, 18.0 mmol) in 20 ml of water a solution of triphosgene (5.34 g, 18.0 mmol) in 20 ml of toluene was added dropwise. A white solid was formed which dissolved by addition of water. The organic phase was eliminated and the water was neutralized with an aqueous solution of NaOH (10%). The white solid formed was filter off, wash with distilled water and recrystallized from abs. EtOH to afford 1.4 g of **14** as a white solid.

Yield (%) 48; m.p.= 132-136°C; I.R.: (nujol, cm<sup>-1</sup>): 1751, 3257. <sup>1</sup>H-NMR (CDCl<sub>3</sub>/TMS): δ 7.51 (m, 3H arom.), 7.89 (d, 2H arom.), 10.0 (broad s., 1H, NH disappearing on deuteration). MS: m/z 163 [MH<sup>+</sup>].

#### 4.2.5. 4,5-Dihydro-1H-benzo[b]azepin-2(3H)-one **15** [44]

3.00 g (21.0 mmol) of 1-tetralone were dissolved in 120 ml of toluene and cooled with an ice bath at 0°C, under stirring. Sodium azide (2.67 g, 41.0 mmol) was added in one portion and, subsequently, 10.2 ml of H<sub>2</sub>SO<sub>4</sub> conc. were added drop by drop, over a period of 30 minutes. The solution was left to stir overnight, then 82 ml of distilled water were slowly added and the organic phase was separated, dried over anhydrous Na<sub>2</sub>SO<sub>4</sub>, filtrate and evaporated *in vacuo*. The solid residue was crystallized from CH<sub>2</sub>Cl<sub>2</sub>/*n*-hexane (1:1) to afford 2.20 g (14.0 mmol, 76%) of **15** as a white crystalline solid.

Melting point: 138-139°C. <sup>1</sup>H-NMR (CDCl<sub>3</sub>/TMS): δ 2.36 (dq, 2H, H<sub>4,4'</sub> CH<sub>2</sub> benzoaz.); 2.49 (q, 2H, H<sub>3,3'</sub> CH<sub>2</sub> benzoaz.); 2.93 (t, 2H, H<sub>5,5'</sub> benzoaz.); 7.09 (d, 1H, H<sub>6</sub> arom.); 7.29 (t, 1H, H<sub>7</sub> arom.); 7.37 (m, 2H, H<sub>8</sub> e H<sub>9</sub> arom.); 7.60 (broad s., 1H, NH-CO disappearing on deuteration).

Compounds **16-22** are commercially available.

#### 4.2.6 General synthesis of intermediate **23-32**

##### 4.2.6.1 (*R,S*) 3-(4-bromobutyl)-4-phenyloxazolidin-2-one **23**

To a solution of 1.6 g (10.0 mmol) of (*R,S*) 4-phenyloxazolin-2-one (**13**), 3.4 g (25.0 mmol) of  $K_2CO_3$  and a catalytic amount of KI in acetonitrile, 5.4 g (25.0 mmol) of 1,4-dibromobutane were slowly added drop by drop stirring at rt. The mixture was then heated under reflux for 6-12h, monitored by TLC ( $CH_2Cl_2/EtOH$  9:1). The hot solution was filtered and evaporated under reduced pressure. The yellow oil residue of (*R,S*) 3-(4-bromobutyl)-4-phenyloxazolidin-2-one **23** was used without further purification.

Yield: 96%; I.R.: (nujol,  $cm^{-1}$ ): 1735;  $^1H$ -NMR ( $CDCl_3/TMS$ ):  $\delta$  1.42 (m, 2H,  $N-CH_2CH_2CH_2CH_2Br$ ); 1.60 (m, 2H,  $N-CH_2CH_2CH_2CH_2Br$ ); 2.65 (m, 1H,  $H_{\square}$ ,  $N-CH_2(CH_2)_3Br$ ); 3.20 (m, 3H,  $H_{\square}$ ,  $N-CH_2(CH_2)_3Br + N-(CH_2)_3CH_2Br$ ); 3.97 (dd, 1H,  $CH_2$  oxad.,  $J= 8.8; 6.6$  Hz); 4.46 (dd 1H, CH oxad.,  $J= 8.8; 8.8$  Hz); 4.62 (dd, 1H,  $CH_2$  oxad.,  $J= 8.8; 6.6$  Hz).

In the same way the enantiomerically pure compounds (**R**)-**23**, (**S**)-**23** and compounds **24-32** were obtained.

##### 4.2.6.2 (*R*) 3-(4-bromobutyl)-4-phenyloxazolidin-2-one (**R**)-**23**

Trituration with petroleum ether ( $40^{\circ}$ - $70^{\circ}$ ) give a yellow oil; yield: 57%;  $^1H$ -NMR: ( $CDCl_3-TMS$ )  $\delta$ : 1.29 (m, 2H,  $N-CH_2CH_2CH_2CH_2Br$ ); 1.50 (m, 2H,  $N-CH_2CH_2CH_2CH_2Br$ ); 2.54 (m, 1H,  $H_{\square}$ ,  $N-CH_2(CH_2)_3Br$ ); 3.10 (m, 3H,  $H_{\square}$ ,  $N-CH_2(CH_2)_3Br + N-(CH_2)_3CH_2Br$ ); 3.80 (m, 1H,  $CH_2$  oxad.); 4.35 (m 1H, CH oxad.); 4.62 (m, 1H,  $CH_2$  oxad.).

##### 4.2.6.3 (*S*) 3-(4-bromobutyl)-4-phenyloxazolidin-2-one (**S**)-**23**

Trituration with petroleum ether ( $40^{\circ}$ - $70^{\circ}$ ) give a yellow oil; yield: 40%;  $^1H$ -NMR: ( $CDCl_3-TMS$ ),  $\delta$ : 1.29 (m, 2H,  $N-CH_2CH_2CH_2CH_2Br$ ); 1.50 (m, 2H,  $N-CH_2CH_2CH_2CH_2Br$ ); 2.54 (m, 1H,  $H_{\square}$ ,  $N-CH_2(CH_2)_3Br$ ); 3.10 (m, 3H,  $H_{\square}$ ,  $N-CH_2(CH_2)_3Br + N-(CH_2)_3CH_2Br$ ); 3.80 (m, 1H,  $CH_2$  oxad.); 4.35 (m 1H, CH oxad.); 4.62 (m, 1H,  $CH_2$  oxad.).

##### 4.2.6.4 3-(4-bromobutyl)-5-Phenyl-1,3,4-oxadiazol-2(3H)-one **24**

White solid (upon cooling overnight), yield: 53%; m.p.  $60-66^{\circ}C$ ;  $^1H$ -NMR: ( $CDCl_3/TMS$ )  $\delta$ : 1.97-2.00 (m, 4H,  $N-CH_2CH_2CH_2CH_2Br$ ), 3.48 (m, 2H,  $N-CH_2CH_2CH_2CH_2Br$ ), 3.83 (m, 2H,  $N-CH_2CH_2CH_2CH_2Br$ ), 7.48 (m, 3H, Ph), 7.85 (m, 2H, Ph).

4.2.6.5 1-(4-bromobutyl)-3,4-dihydroquinolin-2(1H)-one **25**

Chromatography column (AcOEt-EtOH 95:5); yellow oil; yield: 92%; <sup>1</sup>H-NMR: (CDCl<sub>3</sub>/TMS) δ: 1.75-1.80 (m, 2H, NCH<sub>2</sub>CH<sub>2</sub>CH<sub>2</sub>CH<sub>2</sub>Br), 1.95-2.00 (m, 2H, NCH<sub>2</sub>CH<sub>2</sub>CH<sub>2</sub>CH<sub>2</sub>Br), 2.60 (t, 2H, CH<sub>2</sub>CH<sub>2</sub>CO dihydroq., *J* = 8 Hz) 2.85 (t, 2H, CH<sub>2</sub>CH<sub>2</sub>CO dihydroq., *J* = 8 Hz), 3.40 (t, 2H, N-CH<sub>2</sub>CH<sub>2</sub>CH<sub>2</sub>CH<sub>2</sub>Br), 3.93 (t, 2H, NCH<sub>2</sub>CH<sub>2</sub>CH<sub>2</sub>CH<sub>2</sub>Br), 6.96-7.23 (m, 4H arom.).

4.2.6.6 4-(4-bromobutyl)-2H-benzo[b][1,4]oxazin-3(4H)-one **26**

Yellow oil; yield: 92%; <sup>1</sup>H-NMR: (CDCl<sub>3</sub>/TMS) δ: 1.77-1.90 (m, 4H, N-CH<sub>2</sub>CH<sub>2</sub>CH<sub>2</sub>CH<sub>2</sub>Br); 3.39 (t, 2H, N-(CH<sub>2</sub>)<sub>3</sub>CH<sub>2</sub>Br); 3.90 (m, 2H, N-CH<sub>2</sub>(CH<sub>2</sub>)<sub>3</sub>Br); 4.51 (m, 2H, H<sub>3-3'</sub> CH<sub>2</sub> benzox.); 6.94 (m, 4H, arom.).

4.2.6.7 4-(4-bromobutyl)-2H-benzo[b][1,4]thiazin-3(4H)-one **27**

Yellow oil; yield: 87%; <sup>1</sup>H-NMR: (CDCl<sub>3</sub>/TMS) δ: 1.75-1.85 (m, 4H, N-CH<sub>2</sub>CH<sub>2</sub>CH<sub>2</sub>CH<sub>2</sub>Br); 3.32 (t, 2H, N-(CH<sub>2</sub>)<sub>3</sub>CH<sub>2</sub>Br); 3.40 (s, 2H, H<sub>3-3'</sub> CH<sub>2</sub> benzothiaz.); 4.00 (t, 2H, N-CH<sub>2</sub>(CH<sub>2</sub>)<sub>3</sub>Br); 6.99-7.34 (m, 4H, arom.).

4.2.6.8 1-(4-bromobutyl)-2,3,4,5-tetrahydro-1H-benzo[b]azepin-2(3H)-one **28**

Orange oil; yield: 76%; <sup>1</sup>H-NMR: (CDCl<sub>3</sub>/TMS) δ: 1.53-1.72 (m, 4H, N-CH<sub>2</sub>CH<sub>2</sub>CH<sub>2</sub>CH<sub>2</sub>Br); 1.90-2.10 (m, 4H, H<sub>3-3'</sub>-H<sub>4-4'</sub> 2xCH<sub>2</sub> benzoaz.); 2.58 (m, 2H, H<sub>5-5'</sub> CH<sub>2</sub> benzoaz.); 3.22 (t, 2H, N-(CH<sub>2</sub>)<sub>3</sub>CH<sub>2</sub>Br); 3.76 (m, 2H, N-CH<sub>2</sub>(CH<sub>2</sub>)<sub>3</sub>Br); 7.03-7.17 (m, 4H, arom.).

4.2.6.9 2-(4-bromobutyl)isoindoline-1,3-dione **29**

This compound has been synthesized starting from potassium phthalimide (1 eq.) and 1,4-dibromobutane (2.5 eq.) by refluxing the mixture in acetone for 6 hours. The hot solution was filtered off from inorganic salts then concentrated *in vacuo* and recrystallized from *n*-hexane to afford a white solid.

Yield: 80%; m.p. 78-82 °C; <sup>1</sup>H-NMR (CDCl<sub>3</sub>/TMS) δ: 1.85 (m, 4H, N-CH<sub>2</sub>CH<sub>2</sub>CH<sub>2</sub>CH<sub>2</sub>Br), 3.43 (t, 2H, N-CH<sub>2</sub>CH<sub>2</sub>CH<sub>2</sub>CH<sub>2</sub>Br), 3.71 (t, 2H, N-CH<sub>2</sub>CH<sub>2</sub>CH<sub>2</sub>CH<sub>2</sub>Br), 7.72 (m, 2H, H<sub>4</sub>, H<sub>7</sub>), 7.82 (m, 2H, H<sub>5</sub>, H<sub>6</sub>).

4.2.6.10 1-(4-bromobutyl)indoline-2,3-dione **30**

To a solution (1eq.) of isoindolin-1,3-dione in DMF, 1.2eq. of NaH (95%) was added at 0°C and the mixture was stirred for 30 minutes. Then 2.5eq. of 1,4-dibromobutane was slowly added and the mixture was allowed to stir at room temperature overnight. The solution was poured into ice-cold water and extracted three times with diethyl ether which was collected, dried over anhydrous Na<sub>2</sub>SO<sub>4</sub>, filtered and evaporated. The residue was purified by chromatography column (100% CH<sub>2</sub>Cl<sub>2</sub>).

Orange oil; yield: 85%; m.p. 76-80 °C; I.R.: (nujol,  $\text{cm}^{-1}$ ): 1610, 1737;  $^1\text{H-NMR}$  ( $\text{CDCl}_3/\text{TMS}$ )  $\delta$ : 1.91 (m, 4H,  $\text{NCH}_2\text{CH}_2\text{CH}_2\text{CH}_2\text{Br}$ ), 3.46 (t, 2H,  $\text{NCH}_2\text{CH}_2\text{CH}_2\text{CH}_2\text{Br}$ ), 3.76 (t, 2H,  $\text{NCH}_2\text{CH}_2\text{CH}_2\text{CH}_2\text{Br}$ ), 6.92 (d, 1H,  $\text{H}_7$ , indol.), 7.12 (t, 1H,  $\text{H}_5$ , indol.), 7.59 (m, 2H,  $\text{H}_4$ ,  $\text{H}_6$  indol.).

#### 4.2.6.11 1-(4-bromobutyl)piperidin-2-one **31**

The synthesis of this intermediate started from 1 eq. of piperidin-2-one dissolved in ACN, 5% mol of TBAB and 1.5eq. of  $\text{CsCO}_3$  as base. The reaction mixture was allowed to stir overnight at room temperature then the solvent was evaporated under reduced pressure. The residue was dissolved with  $\text{CH}_2\text{Cl}_2$  and washed with water 3 times. The oily residue was purified by chromatography column on silica gel (eluent: AcOEt/EtOH 95-5).

Yield: 15%;  $^1\text{H-NMR}$  ( $\text{CDCl}_3\text{-TMS}$ ),  $\delta$ : 1.54-1.77 (m, 8H, (4)  $\text{CH}_2\text{CH}_2\text{CH}_2\text{CH}_2$  and (4)  $\text{NCH}_2\text{CH}_2\text{CH}_2\text{CH}_2\text{CO}$  pip.), 2.24 (m, 2H,  $\text{NCH}_2\text{CH}_2\text{CH}_2\text{CH}_2\text{CO}$  pip.), 3.13-3.30 (m, 4H, (2)  $\text{CH}_2\text{CH}_2\text{CH}_2\text{CH}_2\text{N}$  and (2)  $\text{NCH}_2\text{CH}_2\text{CH}_2\text{CH}_2\text{CO}$  pip.), 3.35 (m, 2H,  $\text{CH}_2\text{CH}_2\text{CH}_2\text{CH}_2\text{Br}$ ).

#### 4.2.6.12 1-(4-bromobutyl)indole **32**

The synthesis of this compound was carried out with the same procedure described above for the corresponding indolin-2,3-dione derivative (**30**), with the addition of a catalytic amount (5% mol) of TBAB into the reaction mixture. The product was purified by chromatography column on silica gel using petroleum ether (40°-70°) as eluent to afford a light yellow oil.

Yield: 23%;  $^1\text{H-NMR}$  ( $\text{CDCl}_3/\text{TMS}$ )  $\delta$ : 1.85 (m, 2H,  $\text{NCH}_2\text{CH}_2\text{CH}_2\text{CH}_2\text{Br}$ ), 2.01 (m, 2H,  $\text{NCH}_2\text{CH}_2\text{CH}_2\text{CH}_2\text{Br}$ ), 3.37 (t, 2H,  $\text{NCH}_2\text{CH}_2\text{CH}_2\text{CH}_2\text{Br}$ ), 4.17 (t, 2H,  $\text{NCH}_2\text{CH}_2\text{CH}_2\text{CH}_2\text{Br}$ ), 6.50 (d, 1H,  $\text{H}_3$ , indol.,  $J= 2.8$  Hz), 7.09 (t, 1H,  $\text{H}_2$ , indol.,  $J= 2.8$  Hz), 7.11 (t, 1H,  $\text{H}_5$ , indol.), 7.21 (t, 1H,  $\text{H}_6$ , indol.), 7.34 (d, 1H,  $\text{H}_4$  indol.), 7.63 (d, 1H,  $\text{H}_7$  indol.).

### 4.2.7 General synthesis of final compounds **2-11a,b**

#### 4.2.7.1 (R,S) 3-(4-Benzyl-(methyl)-amino)-butyl)-4-phenyl-oxazolidin-2-one **2a**

A solution of 0.17 g (1.40 mmol) of N-benzylmethylamine, 0.20 g (1.40 mmol) of  $\text{K}_2\text{CO}_3$  and 0.40 g of (R,S)-3-(4-bromobutyl)-5-phenyloxazolidin-2-one **23** in ACN was allowed to stirring under reflux for 6-12 h and monitored by TLC until the reaction was completed. The hot

solution was filtered and concentrated *in vacuo* to afford 0.29 g (85.0 mmol) of a chromatography pure yellow oil **2a**.

I.R.: (nujol,  $\text{cm}^{-1}$ ) 1754 (C=O);  $^1\text{H-NMR}$ : ( $\text{CDCl}_3$ -TMS; 200 MHz),  $\delta$ : 1.40-1.60 (m, 4H,  $\text{CH}_2\text{CH}_2\text{CH}_2\text{CH}_2$ ); 2.14 (s, 3H,  $\text{NCH}_3$ ); 2.32 (t, 2H,  $(\text{CH}_2)_3\text{CH}_2\text{NCH}_3$ ); 2.80 (m, 1H,  $\text{H}_a$ ,  $\text{NCH}_2(\text{CH}_3)_3\text{NCH}_3$ ); 3.43 (m, 3H,  $\text{H}_b$ ,  $\text{NCH}_2(\text{CH}_2)_3\text{NCH}_3$  + (2)  $\text{N}(\text{CH}_3)\text{CH}_2\text{Ph}$ ); 4.11 (dd, 1H,  $\text{CH}_2$  oxad.;  $J= 8.8$ ; 6.6 Hz); 4.60 (t, 1H, CH oxad.  $J= 8.8$ ; 8.8 Hz); 4.77 (dd, 1H,  $\text{CH}_2$  oxad.  $J= 8.8$ ; 6.6 Hz); 7.20-7.40 (m, 10H, arom). MS:  $m/z$  339 [ $\text{MH}^+$ ].

The 1-(4-chlorophenyl)-*N*-methylethylmethanamine was synthesized starting from 4-chlorobenzyl chloride (14.0 mmol) and 20 ml of ethanolic solution of methylamine (33%) under reflux for 2h. The mixture was distilled under vacuum to eliminate the excess of methylamine and washed with a saturated  $\text{NaHCO}_3$  solution to afford a yellow oil (56%) that was used without further purification.

The 1-(2,4-dimethylphenyl)-*N*-methylethylmethanamine was synthesized in analogous way.

#### 4.2.7.2 (*R,S*) 3-(4-((4-Chlorobenzyl)-(methyl)-amino)-butyl)-4-phenyl-oxazolidin-2-one **2b**.

Starting from 1-(4-chlorophenyl)-*N*-methylethylmethanamine and (*R,S*)-3(4-bromobutyl)-5-phenyloxazolidin-2-one **23** following the same procedure described above, 70% of **2b** was obtained as a yellow pure oil.

I.R.: (nujol,  $\text{cm}^{-1}$ ) 1754 (C=O).  $^1\text{H-NMR}$ : ( $\text{CDCl}_3$ -TMS; 200 MHz)  $\delta$ : 1.30-1.50 (m, 4H,  $\text{CH}_2\text{CH}_2\text{CH}_2\text{CH}_2$ ); 2.11 (s, 3H,  $\text{NCH}_3$ ); 2.30 (m, 1H,  $(\text{CH}_2)_3\text{CH}_2\text{NCH}_3$ ); 2.80 (m, 1H,  $(\text{CH}_2)_3\text{CH}_2\text{NCH}_3$ ); 3.38 (s, 2H,  $\text{NCH}_2(\text{CH}_2)_3\text{NCH}_3$ ); 3.45 (s, 2H,  $\text{N}(\text{CH}_3)\text{CH}_2\text{Ph}$ ); 4.10 (dd, 1H,  $\text{CH}_2$  oxad.;  $J= 8.0$ ; 6.0 Hz); 4.59 (t, 1H, CH oxad.;  $J= 8.0$ ; 8.0 Hz); 4.78 (dd, 1H,  $\text{CH}_2$  oxad.;  $J= 8.0$ ; 6.0 Hz); 7.20-7.40 (m, 9H, arom). MS:  $m/z$  371 [ $\text{MH}^+$ ], 373 [ $\text{MH}^++2$ ].

Following the same procedure described above, compounds (**R**)-**2a,b**, (**S**)-**2a,b** and **3-11a,b** were obtained.

#### 4.2.7.3 (*R*) 3-(4-Benzyl-(methyl)-amino)-butyl)-4-phenyl-oxazolidin-2-one (**R**)-**2a**

Yellow oil; yield: 83%; I.R.: (nujol,  $\text{cm}^{-1}$ ) 1754 (C=O).  $^1\text{H-NMR}$ : ( $\text{CDCl}_3$ -TMS; 400 MHz)  $\delta$ : 1.20-1.40 (m, 4H,  $\text{CH}_2\text{CH}_2\text{CH}_2\text{CH}_2$ ); 1.99 (s, 3H,  $\text{NCH}_3$ ); 2.19 (t, 2H,  $(\text{CH}_2)_3\text{CH}_2\text{NCH}_3$ ); 2.65 (m, 1H,  $\text{N-CH}_2(\text{CH}_3)_3\text{NCH}_3$ ); 3.30 (m, 3H,  $\text{N}(\text{CH}_3)\text{CH}_2\text{Ph}$  + 1H  $\text{N-CH}_2(\text{CH}_2)_3\text{NCH}_3$ ); 3.93 (m,

1H, CH oxad.;  $J= 12.0; 8.0$  Hz); 4.45 (t, 1H, CH<sub>2</sub> oxad.  $J= 12.0; 12.0$  Hz); 4.65 (m, 1H, CH<sub>2</sub> oxad.  $J= 12.0; 8.0$  Hz); 7.15-7.25 (m, 10H, arom). MS: m/z 339 [MH<sup>+</sup>].

#### 4.2.7.4 (R) 3-(4-((4-Chlorobenzyl)-(methyl)-amino)-butyl)-4-phenyl-oxazolidin-2-one (R)-2b

Yellow oil; yield: 82%; I.R.: (nujol, cm<sup>-1</sup>) 1754 (C=O). <sup>1</sup>H-NMR: (CDCl<sub>3</sub>-TMS; 400 MHz)  $\delta$ : 1.30-1.50 (m, 4H, CH<sub>2</sub>CH<sub>2</sub>CH<sub>2</sub>CH<sub>2</sub>); 2.06 (s, 3H, NCH<sub>3</sub>); 2.24 (m, 1H, (CH<sub>2</sub>)<sub>3</sub>CH<sub>2</sub>NCH<sub>3</sub>); 2.75 (m, 1H, (CH<sub>2</sub>)CH<sub>2</sub>NCH<sub>3</sub>); 3.34 (s, 2H, N(CH<sub>3</sub>)CH<sub>2</sub>Ph); 3.42 (m, 2H, NCH<sub>2</sub>(CH<sub>2</sub>)<sub>3</sub>NCH<sub>3</sub>); 4.05 (m, 1H, CH<sub>2</sub> oxad.;  $J= 12.0; 8.0$  Hz); 4.55 (t, 1H, CH oxad.;  $J= 12.0; 12.0$  Hz); 4.74 (t, 1H, CH<sub>2</sub> oxad.;  $J= 12.0; 8.0$  Hz); 7.13-7.43 (m, 9H, arom). MS: m/z 371 [MH<sup>+</sup>], 373 [MH<sup>+</sup>+2].

#### 4.2.7.5 (S) 3-(4-Benzyl-(methyl)-amino)-butyl)-4-phenyl-oxazolidin-2-one (S)-2a

Yellow oil; yield: 91%; I.R.: (nujol, cm<sup>-1</sup>) 1754 (C=O). <sup>1</sup>H-NMR: (CDCl<sub>3</sub>-TMS; 500 MHz)  $\delta$ : 1.40-1.50 (m, 4H, CH<sub>2</sub>CH<sub>2</sub>CH<sub>2</sub>CH<sub>2</sub>); 2.11 (s, 3H, NCH<sub>3</sub>); 2.30 (t, 2H, (CH<sub>2</sub>)<sub>3</sub>CH<sub>2</sub>NCH<sub>3</sub>); 2.77 (m, 1H, NCH<sub>2</sub>(CH<sub>3</sub>)<sub>3</sub>NCH<sub>3</sub>); 3.41 (m, 3H, N(CH<sub>3</sub>)CH<sub>2</sub>Ph + 1H N-CH<sub>2</sub>(CH<sub>2</sub>)<sub>3</sub>NCH<sub>3</sub>); 4.08 (dd, 1H, CH<sub>2</sub> oxad.;  $J= 10.0; 5.0$  Hz); 4.57 (t, 1H, CH oxad.  $J= 10.0; 5.0$  Hz); 4.76 (dd, 1H, CH<sub>2</sub> oxad.  $J= 10.0; 5.0$  Hz); 7.25-7.40 (m, 10H, arom). MS: m/z 339 [MH<sup>+</sup>].

#### 4.2.7.6 (L) 3-(4-((4-Chlorobenzyl)-(methyl)-amino)-butyl)-4-phenyl-oxazolidin-2-one (S)-2b

Yellow oil; yield: 83%; I.R.: (nujol, cm<sup>-1</sup>) 1754 (C=O). <sup>1</sup>H-NMR: (CDCl<sub>3</sub>-TMS; 500 MHz)  $\delta$ : 1.30-1.45 (m, 4H, CH<sub>2</sub>CH<sub>2</sub>CH<sub>2</sub>CH<sub>2</sub>); 2.09 (s, 3H, NCH<sub>3</sub>); 2.27 (m, 1H, (CH<sub>2</sub>)<sub>3</sub>CH<sub>2</sub>NCH<sub>3</sub>); 2.77 (m, 1H, (CH<sub>2</sub>)<sub>3</sub>CH<sub>2</sub>NCH<sub>3</sub>); 3.36 (s, 2H, N(CH<sub>3</sub>)CH<sub>2</sub>Ph); 3.40 (m, 2H, NCH<sub>2</sub>(CH<sub>2</sub>)<sub>3</sub>NCH<sub>3</sub>); 4.06 (dd, 1H, CH<sub>2</sub> oxad.;  $J= 10.0; 5.0$  Hz); 4.57 (t, 1H, CH oxad.;  $J= 10.0; 5.0$  Hz); 4.76 (dd, 1H, CH<sub>2</sub> oxad.;  $J= 10.0; 10.0$  Hz); 7.20-7.40 (m, 9H, arom). MS: m/z 371 [MH<sup>+</sup>], 373 [MH<sup>+</sup>+2].

#### 4.2.7.7 3-(4-(Benzyl(methyl)amino)butyl)-5-phenyl-1,3,4-oxadiazol-2(3H)-one 3a

Yellow oil; yield: 91%; I.R.: (nujol, cm<sup>-1</sup>) 1787 (C=O). <sup>1</sup>H-NMR: (CDCl<sub>3</sub>-TMS; 200 MHz)  $\delta$ : 1.58-1.83 (m, 4H, CH<sub>2</sub>CH<sub>2</sub>CH<sub>2</sub>CH<sub>2</sub>); 2.17 (s, 3H, NCH<sub>3</sub>); 2.43 (t, 2H, (CH<sub>2</sub>)<sub>3</sub>CH<sub>2</sub>NCH<sub>3</sub>); 3.47 (s, 2H, N(CH<sub>3</sub>)CH<sub>2</sub>Ph); 3.76 (t, 2H, NCH<sub>2</sub>(CH<sub>3</sub>)<sub>3</sub>NCH<sub>3</sub>); 7.28-7.82 (m, 10H, arom). MS: m/z 338 [MH<sup>+</sup>].

#### 4.2.7.8 3-(4-((4-Chlorobenzyl)(methyl)amino)butyl)-5-phenyl-1,3,4-oxadiazol-2(3H)-one 3b

Yellow oil; yield: 47%; I.R.: (nujol, cm<sup>-1</sup>) 1775 (C=O). <sup>1</sup>H-NMR: (CDCl<sub>3</sub>-TMS; 200 MHz)  $\delta$ : 1.90-2.00 (m, 4H, CH<sub>2</sub>CH<sub>2</sub>CH<sub>2</sub>CH<sub>2</sub>); 2.15 (s, 3H, NCH<sub>3</sub>); 3.43 (m, 4H, (CH<sub>2</sub>)<sub>3</sub>CH<sub>2</sub>N(CH<sub>3</sub>)CH<sub>2</sub>Ph); 3.82 (t, 2H, NCH<sub>2</sub>(CH<sub>3</sub>)<sub>3</sub>NCH<sub>3</sub>); 7.26-7.83 (m, 9H, arom). MS: m/z 371 [MH<sup>+</sup>], 373 [MH<sup>+</sup>+2].

4.2.7.13 1-(4-(Benzyl(methyl)amino)butyl)-3,4-dihydroquinolin-2(1H)-one **4a**

Yellow oil; yield: 80%; I.R.: (nujol,  $\text{cm}^{-1}$ ) 1634 (C=O).  $^1\text{H-NMR}$ : ( $\text{CDCl}_3$ -TMS; 200 MHz)  $\delta$ : 1.50-1.70 (m, 4H,  $\text{CH}_2\text{CH}_2\text{CH}_2\text{CH}_2$ ); 2.00 (s, 3H, N- $\text{CH}_3$ ); 2.27 (t, 2H, N- $\text{CH}_2\text{CH}_2\text{CH}_2\text{CH}_2$ ); 2.49 (t, 2H,  $\text{CH}_2\text{CH}_2$ -CO dihydroq.,  $J= 8.0$  Hz); 2.71 (t, 2H,  $\text{CH}_2\text{CH}_2$ -CO dihydroq.,  $J= 8.0$  Hz); 3.30 (s, 2H, Ph $\text{CH}_2\text{N}$ ); 3.77 (t, 2H, N- $\text{CH}_2(\text{CH}_2)_3$ -N- $\text{CH}_3$ ); 6.80-7.20 (m, 9H, arom). MS: m/z 323 [ $\text{MH}^+$ ].

4.2.7.14 1-(4-((4-Chlorobenzyl)(methyl)amino)butyl)-3,4-dihydroquinolin-2(1H)-one **4b**

Yellow oil; yield: 73%; I.R.: (nujol,  $\text{cm}^{-1}$ ) 1679 (C=O).  $^1\text{H-NMR}$ : ( $\text{CDCl}_3$ -TMS; 200 MHz)  $\delta$ : 1.55-1.68 (m, 4H,  $\text{CH}_2\text{CH}_2\text{CH}_2\text{CH}_2$ ); 2.24 (s, 3H, N- $\text{CH}_3$ ); 2.54 (t, 2H,  $(\text{CH}_2)_3$ - $\text{CH}_2$ -N- $\text{CH}_3$ ); 2.64 (t, 2H,  $\text{CH}_2\text{CH}_2$ -CO chin.,  $J= 8$  Hz); 2.88 (t, 2H,  $\text{CH}_2\text{CH}_2$ -CO chin.,  $J= 8$  Hz); 3.55 (s, 2H, Ph $\text{CH}_2\text{N}$ ); 3.95 (t, 2H, N- $\text{CH}_2\text{CH}_2\text{CH}_2\text{CH}_2$ -NCO); 6.90-7.30 (m, 8H, arom). MS: m/z 357 [ $\text{MH}^+$ ], 359 [ $\text{MH}^++2$ ].

4.2.7.15 2-(4-Benzyl(methyl)amino)butyl)-2H-benzo[b][1,4]oxazin-3(4H)-one **5a**

Yellow oil; yield: 88%; I.R.: (nujol,  $\text{cm}^{-1}$ ) 1695 (C=O).  $^1\text{H-NMR}$ : ( $\text{CDCl}_3$ -TMS; 400 MHz)  $\delta$ : 1.50-1.60 (m, 4H,  $\text{CH}_2\text{CH}_2\text{CH}_2\text{CH}_2$ ); 2.05 (s, 3H, N $\text{CH}_3$ ); 2.29 (m, 2H,  $(\text{CH}_2)_3\text{CH}_2\text{NCH}_3$ ); 3.33 (s, 2H, N $\text{CH}_2\text{Ph}$ ); 3.79 (m, 2H,  $\text{CH}_2(\text{CH}_2)_3\text{NCH}_3$ ); 4.40 (s, 2H,  $\text{H}_{3,3'}$ - $\text{CH}_2$  benzox.); 6.85 (m, 4H, arom. benzox.); 7.16 (m, 5H, arom. Ph). MS: m/z 325 [ $\text{MH}^+$ ].

4.2.7.16 2-(4-((4-Chlorobenzyl)(methyl)amino)butyl)-2H-benzo[b][1,4]oxazin-3(4H)-one **5b**

Yellow oil; yield: 88%; I.R.: (nujol,  $\text{cm}^{-1}$ ) 1682 (C=O).  $^1\text{H-NMR}$ : ( $\text{CDCl}_3$ -TMS; 400 MHz)  $\delta$ : 1.46-1.60 (m, 4H,  $\text{CH}_2\text{CH}_2\text{CH}_2\text{CH}_2$ ); 2.04 (s, 3H, N $\text{CH}_3$ ); 2.30 (m, 1H,  $(\text{CH}_2)_3\text{CH}_2\text{NCH}_3$ ); 3.33 (s, 3H, N $\text{CH}_2\text{Ph}$  e  $(\text{CH}_2)_3\text{CH}_2\text{NCH}_3$ ); 3.78 (m, 2H,  $\text{CH}_2(\text{CH}_2)_3\text{NCH}_3$ ); 4.41 (s, 2H,  $\text{H}_{3,3'}$ - $\text{CH}_2$  benzox.); 6.85 (m, 4H, arom. benzox.); 7.12 (m, 4H, arom. Ph). MS: m/z 359 [ $\text{MH}^+$ ], 361 [ $\text{MH}^++2$ ].

4.2.7.17 2-(4-Benzyl(methyl)amino)butyl)-2H-benzo[b][1,4]thiazin-3(4H)-one **6a**

Yellow oil; yield: 38%; I.R.: (nujol,  $\text{cm}^{-1}$ ) 1674 (C=O).  $^1\text{H-NMR}$ : ( $\text{CDCl}_3$ -TMS; 400 MHz)  $\delta$ : 1.49-1.59 (m, 4H,  $\text{CH}_2\text{CH}_2\text{CH}_2\text{CH}_2$ ); 2.09 (s, 3H, N $\text{CH}_3$ ); 2.33 (m, 1H,  $(\text{CH}_2)_3\text{CH}_2\text{NCH}_3$ ); 3.21-3.24 (m, 3H, N $\text{CH}_2\text{Ph}$  e 1H  $(\text{CH}_2)_3\text{CH}_2\text{NCH}_3$ ); 3.40 (s, 2H,  $\text{H}_{3,3'}$ - $\text{CH}_2$  benzothiaz.); 3.91 (m, 2H,  $-\text{CH}_2(\text{CH}_2)_3$ -N- $\text{CH}_3$ ); 6.90-7.20 (m, 9H, arom. benzothiaz. and Ph). MS: m/z 341 [ $\text{MH}^+$ ];

4.2.7.18 2-(4-((4-Chlorobenzyl)(methyl)amino)butyl)-2H-benzo[b][1,4]thiazin-3(4H)-one **6b**

Yellow oil; yield: 52%; I.R.: (nujol,  $\text{cm}^{-1}$ ) 1651 (C=O).  $^1\text{H-NMR}$ : ( $\text{CDCl}_3$ -TMS; 400 MHz)  $\delta$ : 1.42-1.54 (m, 4H,  $\text{CH}_2\text{CH}_2\text{CH}_2\text{CH}_2$ ); 2.02 (s, 3H, N $\text{CH}_3$ ); 2.27 (m, 1H,  $(\text{CH}_2)_3\text{CH}_2\text{NCH}_3$ ); 3.17-3.20 (m, 3H, N $\text{CH}_2\text{Ph}$  e 1H  $(\text{CH}_2)_3\text{CH}_2\text{NCH}_3$ ); 3.32 (s, 2H,  $\text{H}_{3,3'}$ - $\text{CH}_2$  benzothiaz.); 3.87

(m, 2H,  $\text{CH}_2(\text{CH}_2)_3\text{NCH}_3$ ); 6.87-7.21 (m, 8H, arom. benzothiaz. and Ph). MS: m/z 375  $[\text{MH}^+]$ , 377  $[\text{MH}^++2]$ .

#### 4.2.7.19 1-(4-(Benzyl(methyl)amino)butyl)-4,5-dihydro-1H-benzo[b]azepin-2(3H)-one **7a**

Orange oil; yield: 49%; I.R.: (nujol,  $\text{cm}^{-1}$ ) 1651 (C=O).  $^1\text{H-NMR}$ : ( $\text{CDCl}_3$ -TMS; 400 MHz)  $\delta$ : 1.44-1.61 (m, 6H,  $\text{CH}_2\text{CH}_2\text{CH}_2\text{CH}_2 + \text{H}_{4,4'}$   $\text{CH}_2$  benzoaz.); 2.09 (s, 3H,  $\text{NCH}_3$ ); 2.21 (m, 1H,  $(\text{CH}_2)_3\text{CH}_2\text{NCH}_3$ ); 2.29 (m, 2H,  $\text{H}_{3,3'}$   $\text{CH}_2$  benzoaz.); 2.65 (m, 2H,  $-\text{CH}_2(\text{CH}_2)_3\text{NCH}_3$ ); 3.38 (s, 2H,  $\text{H}_{5,5'}$   $\text{CH}_2$  benzoaz.); 3.43 (s, 2H,  $\text{CH}_2\text{Ph}$ ); 7.14-7.25 (m, 9H, arom. benzoaz. and Ph). MS: m/z 337  $[\text{MH}^+]$ .

#### 4.2.7.20 1-(4-((4-Chlorobenzyl)(methyl)amino)butyl)-4,5-dihydro-1H-benzo[b]azepin-2(3H)-one **7b**

Orange oil; yield: 51%; I.R.: (nujol,  $\text{cm}^{-1}$ ) 1659 (C=O).  $^1\text{H-NMR}$ : ( $\text{CDCl}_3$ -TMS; 400 MHz)  $\delta$ : 1.44-1.62 (m, 6H,  $\text{CH}_2\text{CH}_2\text{CH}_2\text{CH}_2 + \text{H}_{4,4'}$   $\text{CH}_2$  benzoaz.); 2.06 (s, 3H,  $\text{NCH}_3$ ); 2.10 (m, 2H,  $\text{H}_{3,3'}$   $\text{CH}_2$  benzoaz.); 2.20 (m, 2H,  $(\text{CH}_2)_3\text{CH}_2\text{NCH}_3$ ); 2.64 (m, 2H,  $\text{CH}_2(\text{CH}_2)_3\text{NCH}_3$ ); 3.33 (s, 2H,  $\text{CH}_2\text{Ph}$ ); 3.42 (m, 2H,  $\text{H}_{5,5'}$   $\text{CH}_2$  benzoaz.); 7.11-7.24 (m, 8H, arom. benzoaz. and Ph). MS: m/z 371  $[\text{MH}^+]$ , 373  $[\text{MH}^++2]$ .

#### 4.2.7.21 2-(4-Benzyl(methyl)amino)butyl)isoindoline-1,3-dione **8a**

Yellow oil; yield: 63%; I.R.: (nujol,  $\text{cm}^{-1}$ ) 1713 (C=O).  $^1\text{H-NMR}$ : ( $\text{CDCl}_3$ -TMS; 200 MHz)  $\delta$ : 1.52-1.72 (m, 4H,  $\text{CH}_2\text{CH}_2\text{CH}_2\text{CH}_2$ ), 2.15 (s, 3H,  $\text{NCH}_3$ ), 2.44 (m, 2H,  $(\text{CH}_2)_3\text{CH}_2\text{NCH}_3$ ), 3.44 (s, 2H,  $\text{N}(\text{CH}_3)\text{CH}_2\text{Ph}$ ), 3.68 (m, 2H,  $\text{NCH}_2(\text{CH}_2)_3\text{NCH}_3$ ), 7.30 (m, 5H, -Ph), 7.68 (m, 2H,  $\text{H}_4, \text{H}_7$ , isoindol.), 7.83 (m, 2H,  $\text{H}_5, \text{H}_6$  isoindol.). MS: m/z 323  $[\text{MH}^+]$ .

#### 4.2.7.22 2-(4-((4-Chlorobenzyl)(methyl)amino)butyl)isoindoline-1,3-dione **8b**

Yellow oil; yield: 47%; I.R.: (nujol,  $\text{cm}^{-1}$ ) 1715 (C=O).  $^1\text{H-NMR}$ : ( $\text{CDCl}_3$ -TMS; 200 MHz)  $\delta$ : 1.45-1.80 (m, 4H,  $\text{CH}_2\text{CH}_2\text{CH}_2\text{CH}_2$ ), 2.14 (s, 3H,  $\text{NCH}_3$ ), 2.37 (t, 2H,  $\text{N}(\text{CH}_2)_3\text{CH}_2\text{NCH}_3$ ), 3.45 (s, 2H,  $\text{N}(\text{CH}_3)\text{CH}_2\text{Ph}$ ), 3.69 (t, 2H,  $\text{NCH}_2(\text{CH}_2)_3\text{NCH}_3$ ), 7.24 (m, 4H, -Ar), 7.70 (m, 2H,  $\text{H}_4, \text{H}_7$ , isoindol.), 7.83 (m, 2H,  $\text{H}_5, \text{H}_6$  isoindol.). MS: m/z 357  $[\text{MH}^+]$ , 359  $[\text{MH}^++2]$ .

#### 4.2.7.23 1-(4-Benzyl(methyl)amino)butyl)indoline-2,3-dione **9a**

Trituration with diethyl ether give a reddish oil; yield: 67%; I.R.: (nujol,  $\text{cm}^{-1}$ ) 1614, 1781 (C=O).  $^1\text{H-NMR}$ : ( $\text{CDCl}_3$ -TMS; 400 MHz)  $\delta$ : 1.58 (m, 2H,  $\text{CH}_2\text{CH}_2\text{CH}_2\text{CH}_2\text{NCH}_3$ ), 1.74 (m, 2H,  $\text{CH}_2\text{CH}_2\text{CH}_2\text{CH}_2\text{NCH}_3$ ), 2.17 (s, 3H,  $\text{NCH}_3$ ), 2.40 (t, 2H,  $\text{CH}_2\text{CH}_2\text{CH}_2\text{CH}_2\text{NCH}_3$ ), 3.45 (s, 2H,  $\text{PhCH}_2\text{N}$ ), 3.71 (t, 2H,  $\text{CH}_2\text{CH}_2\text{CH}_2\text{CH}_2\text{NCH}_3$ ), 6.86-7.60 (m, 9H, arom.). MS: m/z 323  $[\text{MH}^+]$ .

#### 4.2.7.24 1-(4-((4-Chlorobenzyl)(methyl)amino)butyl)indoline-2,3-dione **9b**

Chromatography column (CH<sub>2</sub>Cl<sub>2</sub>-EtOH 98:2); reddish oil; yield: 95%; I.R.: (nujol, cm<sup>-1</sup>) 1614, 1763 (C=O). <sup>1</sup>H-NMR: (CDCl<sub>3</sub>-TMS; 400 MHz) δ: 1.57 (m, 2H, CH<sub>2</sub>CH<sub>2</sub>CH<sub>2</sub>CH<sub>2</sub>NCH<sub>3</sub>), 1.73 (m, 2H, CH<sub>2</sub>CH<sub>2</sub>CH<sub>2</sub>CH<sub>2</sub>NCH<sub>3</sub>), 2.14 (s, 3H, NCH<sub>3</sub>), 2.38 (t, 2H, CH<sub>2</sub>CH<sub>2</sub>CH<sub>2</sub>CH<sub>2</sub>NCH<sub>3</sub>), 3.41 (s, 2H, PhCH<sub>2</sub>N), 3.71 (t, 2H, CH<sub>2</sub>CH<sub>2</sub>CH<sub>2</sub>CH<sub>2</sub>NCH<sub>3</sub>), 6.86-7.60 (m, 8H, arom.). MS: m/z 357 [MH<sup>+</sup>], 359 [MH<sup>+</sup>+2].

#### 4.2.7.25 1-(4-Benzyl(methyl)amino)butyl)piperidin-2-one **10a**

Yellow oil; yield: 27%; I.R.: (nujol, cm<sup>-1</sup>) 1750 (C=O). <sup>1</sup>H-NMR: (CDCl<sub>3</sub>-TMS; 400 MHz) δ: 1.40-1.55 (m, 4H, CH<sub>2</sub>CH<sub>2</sub>CH<sub>2</sub>CH<sub>2</sub>), 1.70-1.80 (m, 4H, NCH<sub>2</sub>CH<sub>2</sub>CH<sub>2</sub>CH<sub>2</sub>CO pip.), 2.15 (s, 3H, N-CH<sub>3</sub>), 2.33 (m, 4H, (2) NCH<sub>2</sub>CH<sub>2</sub>CH<sub>2</sub>CH<sub>2</sub>N-CH<sub>3</sub> and (2) N-CH<sub>2</sub>CH<sub>2</sub>CH<sub>2</sub>CH<sub>2</sub>NCO pip.), 3.22 (t, 2H, NCH<sub>2</sub>CH<sub>2</sub>CH<sub>2</sub>CH<sub>2</sub>CO pip.), 3.31 (t, 2H, NCH<sub>2</sub>CH<sub>2</sub>CH<sub>2</sub>CH<sub>2</sub>N-CH<sub>3</sub>), 3.44 (s, 2H, PhCH<sub>2</sub>N), 7.20-7.30 (m, 5H, arom.). MS: m/z 275 [MH<sup>+</sup>].

#### 4.2.7.26 1-(4-(4-Chlorobenzyl(methyl)amino)butyl)piperidin-2-one **10b**

Yellow oil; yield: 47%; I.R.: (nujol, cm<sup>-1</sup>) 1751 (C=O). <sup>1</sup>H-NMR: (CDCl<sub>3</sub>-TMS; 400 MHz) δ: 1.43-1.51 (m, 4H, CH<sub>2</sub>CH<sub>2</sub>CH<sub>2</sub>CH<sub>2</sub>), 1.65-1.75 (m, 4H, NCH<sub>2</sub>CH<sub>2</sub>CH<sub>2</sub>CH<sub>2</sub>CO pip.), 2.10 (s, 3H, N-CH<sub>3</sub>), 2.30 (m, 4H, (2) NCH<sub>2</sub>CH<sub>2</sub>CH<sub>2</sub>CH<sub>2</sub>N-CH<sub>3</sub> and (2) N-CH<sub>2</sub>CH<sub>2</sub>CH<sub>2</sub>CH<sub>2</sub>NCO pip.), 3.18 (t, 2H, NCH<sub>2</sub>CH<sub>2</sub>CH<sub>2</sub>CH<sub>2</sub>CO pip.), 3.29 (t, 2H, NCH<sub>2</sub>CH<sub>2</sub>CH<sub>2</sub>CH<sub>2</sub>N-CH<sub>3</sub>), 3.36 (s, 2H, PhCH<sub>2</sub>N), 7.17-7.22 (m, 4H, arom.). MS: m/z 309 [MH<sup>+</sup>], 311 [MH<sup>+</sup>+2].

#### 4.2.7.27 1-(4-Benzyl(methyl)amino)butyl)indole **11a**

Light orange oil; yield: 82%; <sup>1</sup>H-NMR: (CDCl<sub>3</sub>-TMS; 400 MHz) δ: 1.51 (m, 2H, CH<sub>2</sub>CH<sub>2</sub>CH<sub>2</sub>CH<sub>2</sub>NCH<sub>3</sub>), 1.87 (m, 2H, CH<sub>2</sub>CH<sub>2</sub>CH<sub>2</sub>CH<sub>2</sub>NCH<sub>3</sub>), 2.14 (s, 3H, NCH<sub>3</sub>), 2.35 (t, 2H, CH<sub>2</sub>CH<sub>2</sub>CH<sub>2</sub>CH<sub>2</sub>NCH<sub>3</sub>), 3.43 (s, 2H, PhCH<sub>2</sub>N), 4.10 (t, 2H, CH<sub>2</sub>CH<sub>2</sub>CH<sub>2</sub>CH<sub>2</sub>NCH<sub>3</sub>), 6.46 (d, 1H, CH H<sub>3</sub>, indol.), 7.06-7.62 (m, 10H, arom.). MS: m/z 293 [MH<sup>+</sup>].

#### 4.2.7.28 1-(4-(4-Chlorobenzyl(methyl)amino)butyl)indole **11b**

Light yellow; yield: 96%; <sup>1</sup>H-NMR: (CDCl<sub>3</sub>-TMS; 400 MHz) δ: 1.51 (m, 2H, CH<sub>2</sub>CH<sub>2</sub>CH<sub>2</sub>CH<sub>2</sub>NCH<sub>3</sub>), 1.87 (m, 2H, CH<sub>2</sub>CH<sub>2</sub>CH<sub>2</sub>CH<sub>2</sub>NCH<sub>3</sub>), 2.13 (s, 3H, NCH<sub>3</sub>), 2.34 (t, 2H, CH<sub>2</sub>CH<sub>2</sub>CH<sub>2</sub>CH<sub>2</sub>NCH<sub>3</sub>), 3.39 (s, 2H, PhCH<sub>2</sub>N), 4.11 (t, 2H, CH<sub>2</sub>CH<sub>2</sub>CH<sub>2</sub>CH<sub>2</sub>NCH<sub>3</sub>), 6.48 (d, 1H, CH H<sub>3</sub>, indol.), 7.07-7.64 (m, 9H, arom.). MS: m/z 327 [MH<sup>+</sup>], 329 [MH<sup>+</sup>+2].

## 5. Biology evaluation

## 5.1 Radioligand Binding Assays.

### 5.1.1 Materials

The guinea pig brains and rat liver for the  $\sigma_1$  and  $\sigma_2$  receptor binding assays were commercially available (Harlan-Winkelmann, Borcheln, Germany). Homogenizers: Elvehjem Potter (B. Braun Biotech International, Melsungen, Germany) and Soniprep 150, MSE, London, UK). Centrifuges: Cooling centrifuge model Rotina 35R (Hettich, Tuttlingen, Germany) and High-speed cooling centrifuge model Sorvall RC-5C plus (Thermo Fisher Scientific, Langenselbold, Germany). Multiplates: standard 96-well multiplates (Diagonal, Muenster, Germany). Shaker: self-made device with adjustable temperature and tumbling speed (scientific workshop of the institute). Harvester: MicroBeta FilterMate-96 Harvester. Filter: Printed Filtermat Typ A and B. Scintillator: Meltilex (Typ A or B) solid state scintillator. Scintillation analyzer: MicroBeta Trilux (all Perkin Elmer LAS, Rodgau-Jügesheim, Germany).

### 5.1.2 Preparation of membrane homogenates from guinea pig brain:

5 guinea pig brains were homogenized with the potter (500-800 rpm, 10 up-and-down strokes) in 6 volumes of cold 0.32 M sucrose. The suspension was centrifuged at 1200 x g for 10 min at 4 °C. The supernatant was separated and centrifuged at 23500 x g for 20 min at 4 °C. The pellet was resuspended in 5-6 volumes of buffer (50 mM TRIS, pH 7.4) and centrifuged again at 23500 x g (20 min, 4 °C). This procedure was repeated twice. The final pellet was resuspended in 5-6 volumes of buffer and frozen (-80 °C) in 1.5 ml portions containing about 1.5 mg protein/ml.

### 5.1.3 Preparation of membrane homogenates from rat liver:

Two rat livers were cut into small pieces and homogenized with the potter (500-800 rpm, 10 up-and-down strokes) in 6 volumes of cold 0.32 M sucrose. The suspension was centrifuged at 1200 x g for 10 min at 4 °C. The supernatant was separated and centrifuged at 31,000 x g for 20 min at 4 °C. The pellet was suspended in 5-6 volumes of buffer (50 mM TRIS, pH 8.0) and incubated at room temperature for 30 min. After the incubation, the suspension was centrifuged again at 31000 x g for 20 min at 4 °C. The final pellet was resuspended in 5-6 volumes of buffer and stored at -80°C in 1.5 ml portions containing about 2 mg protein/ml.

### 5.1.4 Protein determination

The protein concentration was determined by the method of Bradford [45], modified by Stoscheck [46]. The Bradford solution was prepared by dissolving 5 mg of Coomassie Brilliant Blue G 250 in 2.5 ml of EtOH (95 %, v/v). 10 ml deionized H<sub>2</sub>O and 5 ml phosphoric acid (85%, m/v) were added to this solution, the mixture was stirred and filled to a total volume of 50.0 ml with deionized water. The calibration was carried out using bovine serum albumin as a standard in 9 concentrations (0.1, 0.2, 0.4, 0.6, 0.8, 1.0, 1.5, 2.0 and 4.0 mg/ml). In a 96-well standard multiplate, 10 µL of the calibration solution or 10 µL of the membrane receptor preparation were mixed with 190 µL of the Bradford solution, respectively. After 5 min, the UV absorption of the protein-dye complex at  $\lambda = 595$  nm was measured with a platereader (Tecan Genios, Tecan, Crailsheim, Germany).

#### *5.1.5 General procedures for the binding assays:*

The test compound solutions were prepared by dissolving approximately 10 µmol (usually 2-4 mg) of test compound in DMSO so that a 10 mM stock solution was obtained. To obtain the required test solutions for the assay, the DMSO stock solution was diluted with the respective assay buffer. The filtermats were presoaked in 0.5% aqueous polyethylenimine solution for 2 h at room temperature before use. All binding experiments were carried out in duplicates in the 96-well multiplates. The concentrations given are the final concentration in the assay. Generally, the assays were performed by addition of 50 µL of the respective assay buffer, 50 µL test compound solution in various concentrations ( $10^{-5}$ ,  $10^{-6}$ ,  $10^{-7}$ ,  $10^{-8}$ ,  $10^{-9}$  and  $10^{-10}$  mol/L), 50 µL of corresponding radioligand solution and 50 µL of the respective receptor preparation into each well of the multiplate (total volume 200 µL). The receptor preparation was always added last. During the incubation, the multiplates were shaken at a speed of 500-600 rpm at the specified temperature. Unless otherwise noted, the assays were terminated after 120 min by rapid filtration using the harvester. During the filtration each well was washed five times with 300 µL of water. Subsequently, the filtermats were dried at 95 °C. The solid scintillator was melted on the dried filtermats at a temperature of 95 °C for 5 minutes. After solidifying of the scintillator at room temperature, the trapped radioactivity in the filtermats was measured with the scintillation analyzer. Each position on the filtermat corresponding to one well of the multiplate was measured for 5 min with the [<sup>3</sup>H]-counting protocol. The overall counting efficiency was 20%. The IC<sub>50</sub>-values were calculated with the program GraphPad Prism<sup>®</sup> 3.0 (GraphPad Software, San Diego, CA, USA) by non-linear regression analysis. Subsequently, the IC<sub>50</sub> values were

transformed into  $K_i$ -values using the equation of Cheng and Prusoff [47]. The  $K_i$ -values are given as mean value  $\pm$  SEM from three independent experiments.

## 5.2 Performance of the binding assays

### 5.2.1 $\sigma_1$ receptor

The assay was performed with the radioligand [ $^3\text{H}$ ]-(+)-Pentazocine (22.0 Ci/mmol; Perkin Elmer). The thawed membrane preparation of guinea pig brain cortex (about 100  $\mu\text{g}$  of the protein) was incubated with various concentrations of test compounds, 2 nM [ $^3\text{H}$ ]-(+)-Pentazocine, and TRIS buffer (50 mM, pH 7.4) at 37 °C. The non-specific binding was determined with 10  $\mu\text{M}$  unlabeled (+)-Pentazocine. The  $K_d$ -value of (+)-Pentazocine is 2.9 nM [48].

### 5.2.2 $\sigma_2$ receptor

The assays were performed with the radioligand [ $^3\text{H}$ ]DTG (specific activity 50 Ci/mmol; ARC, St. Louis, MO, USA). The thawed membrane preparations (rat liver preparation containing 100  $\mu\text{g}$  protein) were incubated with various concentrations of the test compound, 3 nM [ $^3\text{H}$ ]DTG and buffer containing (+)-pentazocine (500 nM (+)-pentazocine in 50 mM TRIS, pH 8.0) at room temperature. The non-specific binding was determined with 10  $\mu\text{M}$  non-labeled DTG. The  $K_d$  value is 17.9 nM [49].

## 5.3 Functional assay for determination of $\sigma_1$ -R cytotoxicity

### 5.3.1 Cell cultures

SH-SY5Y (human neuroblastoma) cells were maintained in Dulbecco's modified Eagle's medium (DMEM) Glutamax (Life Technologies) supplemented with 10% (v/v) fetal bovine serum (FBS) and Antibiotic Antimycotic Solution (Sigma-Aldrich, 100 U penicillin, 100  $\mu\text{g}/\text{ml}$  streptomycin and 0.25  $\mu\text{g}/\text{ml}$  amphotericin B) at 37 °C in a humidified incubator with a 5%  $\text{CO}_2/95\%$  air atmosphere.

### 5.3.2 MTT viability assay

The cytotoxic effects of the sigma ligands were evaluated by MTT test on SH-SY5Y cells. Briefly, cells were plated  $1 \times 10^3$  cells/well in 96-well plates 24 h prior to treatment with the

compounds. The compounds were dissolved in DMSO and serially diluted in culture medium to achieve the desired final concentrations. The final concentration of DMSO in the culture medium was always = 1.0%. After 48 h, 20  $\mu$ l MTT solution (5mg/ml) was added to each well, and plates were incubated for 4 h at 37°C. Multiwell plates were then read in a iMark™ Microplate Absorbance Reader (Bio-rad). All compounds were assayed in triplicates, and the results derive from at least three independent experiments. Results are presented by mean absorbance (A595 subtracted by A655)  $\pm$  SD. Statistical analysis was done using one-way ANOVA Test (GraphPad Prism; GraphPad Software, La Jolla, CA).

Cell viability was determined by calculating the mean absorbance of treated samples divided by mean absorbance of respective control (DMSO) and indicated as percentage. Cell cytotoxicity was determined by formula 100 - cell viability (%).

### Acknowledgment

The financial support of FRA 2014 (owner: Dr. Daniele Zampieri) Research Fund University of Trieste-Italy, is gratefully acknowledged.

### References

- [1] W.R. Martin, C.E. Eades, J.A. Thompson, R.E. Huppler, J. Pharmacol. Exp. Ther. 197 (1976) 517-532.
- [2] A.L. Gundlach, B. L. Largent, S. H. Snyder, Eur. J. Pharmacol. 113 (1985) 465–466.
- [3] W.D. Bowen, Pharm. Acta Helv. 74 (2000) 211-218.
- [4] S.B. Hellewell, W.D. Bowen, Brain Res. 527 (1990) 235- 236.
- [5] Y. Itzhak, I. Stein, Brain Res. 599 (1991) 166-172.
- [6] R. Quirion, W.D. Bowen, Y. Itzhak, J.L. Junien, J.M. Mustacchio, R.B. Rothman, T.P. Su, S.W. Tam, D.P. Taylor, Trends Pharmacol. Sci. 13 (1992) 85-86.
- [7] S.B. Hellewell, A. Bruce, G. Feinstein, J. Orringer, W. Williams, W.D. Bowen, Eur. J. Pharmacol. 268 (1994) 9-18.
- [8] F.F. Moebius, J. Striessnig, H. Glossmann, Trends Pharmacol. Sci. 18 (1997) 67-70.
- [9] T.P. Su, T.C. Su, Y. Nakamura, S.Y. Tsai Trends Pharmacol. Sci. 37 (2016) 262-278.
- [10] K.W. Crawford, W.D. Bowen, *Cancer Res.* 62 (2002) 313-322.

- [11] K.W. Crawford, K.W. Coop, W.D. Bowen, *Eur. J. Pharmacol.* 443 (2002) 207-209.
- [12] T. Hayashy, T.P Su, *Proc. Natl. Acad. Sci. USA* 98 (2001) 491-496.
- [13] Z. Wu, W.D. Bowen, *J. Biol. Chem.* 283 (2008) 28198-28215.
- [14] J.M. Walker, W.D. Bowen, F.O. Walker, R.R. Matsumoto, B. De Costa, K.C. Rice, *Pharmacol Rev.* 42 (1990) 355-402.
- [15] D. Fontanilla, M. Johannessen, A.R. Hajipour, N.V. Cozzi, M.B. Jackson, A.E. Ruoho, *Science* 323 (2009) 934-937.
- [16] D. Zampieri, M.G. Mamolo, E. Laurini, C. Zanette, C. Florio, S. Collina, D. Rossi, O. Azzolina, L. Vio, *Eur. J. Med. Chem.* 44 (2009) 124-130.
- [17] D. Zampieri, M.G. Mamolo, E. Laurini, C. Florio, C. Zanette, M. Fermeglia, P. Posocco, M.S. Paneni, S. Pricl, L. Vio, *J. Med. Chem.* 52 (2009) 5380-5393.
- [18] E. Laurini, V. Dal Col, M.G. Mamolo, D. Zampieri, P. Posocco, M. Fermeglia, L. Vio, S. Pricl, *ACS Med. Chem. Lett.* 2 (2011) 834-839.
- [19] E. Laurini, D. Marson, V. Dal Col, M. Fermeglia, M.G. Mamolo, D. Zampieri, L. Vio, S. Pricl, *Mol. Pharm.* 20 (2012) 3107-3126.
- [20] C. Meyer, D. Schepmann, S. Yanagisawa, J. Yamaguchi, V. Dal Col, E. Laurini, K. Itami, S. Pricl, B. Wünsch, *J. Med. Chem.* 55 (2012) 8047-8065.
- [21] D. Rossi, A. Marra, P. Picconi, M. Serra, L. Catenacci, M. Sorrenti, E. Laurini, M. Fermeglia, S. Pricl, S. Brambilla, N. Almirante, M. Peviani, D. Curti, S. Collina, *Bioorg. Med. Chem.* 21 (2013), 21, 2577-2586.
- [22] E. Laurini, V. Dal Col, B. Wünsch, S. Pricl, *Bioorg. Med. Chem. Lett.* 23 (2013) 2868-2871.
- [23] D. Rossi, A. Pedrali, R. Gaggeri, A. Marra, L. Pignataro, E. Laurini, V. Dal Col, M. Fermeglia, S. Pricl, D. Schepmann, B. Wünsch, M. Peviani, D. Curti, S. Collina, *ChemMedChem.* 8 (2013) 1514-1527.
- [24] D. Zampieri, E. Laurini, L. Vio, S. Golob, M. Fermeglia, S. Pricl, M.G. Mamolo, *Bioorg. Med. Chem. Lett.* 24 (2014) 1021-1025.
- [25] F. Weber, S. Brune, K. Korpis, P.J. Bednarski, E. Laurini, V. Dal Col, S. Pricl, D. Schepmann, B. Wünsch, *J. Med. Chem.* 57 (2014) 2884-2894.
- [26] S. Brune, D. Schepmann, K.H. Klempnauer, D. Marson, V. Dal Col, E. Laurini, M.

- Fermeglia, B. Wünsch, S. Pricl, *Biochemistry* 53 (2014) 2993-3003.
- [27] E. Laurini, D. Harel, D. Marson, D. Schepmann, T.J. Schmidt, S. Pricl, B. Wünsch, *Eur. J. Med. Chem.* 83 (2014) 526-533.
- [28] D. Zampieri, E. Laurini, L. Vio, M. Fermeglia, S. Pricl, B. Wünsch, D. Schepmann, M.G. Mamolo, *Eur. J. Med. Chem.* 90 (2015) 797-808.
- [29] M.R. Lee, Y. Duan, P.A. Kollman, *Proteins* 39 (2000) 309-316.
- [30] C. Abate, M. Niso, M. Contino, N.A. Colabufo, S. Ferorelli, R. Perrone, F. Berardi, *ChemMedChem* (2011) 6, 73-80.
- [31] D.T. Aulta, L.L. Werling, *Brain Research* 877 (2000) 354-360.
- [32] W. Hong, S.J. Numayhid, L.L. Werling, *Synapse*, 54 (2004) 102-110.
- [33] W. Hong, L.L. Werling, *Eur. J. Pharmacol.*, 436 (2002) 35-45.
- [34] E.J. Cobos, E. Del Pozo, J.M. Baeyens, *J. Neurochem.* 103(3) (2007) 812-825.
- [35] C. Zeng, J.M. Rothfuss, J. Zhang, S. Vangveravong, W. Chu, S. Li, Z. Tu, J. Xu, R.H. Mach, *Anal Biochem.* 448 (2014) 68-74.
- [36] T. Maurice, T.P. Su, *Pharmacology & therapeutics.* 124 (2009) 195-206.
- [37] G.M. Morris, R. Huey, W. Lindstrom, M.F. Sanner, R.K. Belew, D.S. Goodsell, A.J. Olson, *J. Comput. Chem.* 30 (2009) 2785-2791.
- [38] D.A. Case, T.A. Darden, T.E. Cheatham III, C.L. Simmerling, J. Wang, R.E. Duke, R. Luo, R.C. Walker, W. Zhang, K.M. Merz, B. Roberts, S. Hayik, A. Roitberg, G. Seabra, J. Swails, A.W. Goetz, I. Kolossvary, K.F. Wong, F. Paesani, J. Vanicek, R.M. Wolf, J. Liu, X. Wu, S.R. Brozell, T. Steinbrecher, H. Gohlke, Q. Cai, X. Ye, J. Wang, M.-J. Hsieh, G. Cui, D.R. Roe, D.H. Mathews, M.G. Seetin, R. Salomon-Ferrer, C. Sagui, V. Babin, T. Luchko, S. Gusarov, A. Kovalenko, P.A. Kollman, *AMBER 14*, University of California, San Francisco, 2015.
- [39] W.L. Jorgensen, J. Chandrasekhar, J.D. Madura, R.W. Impey, M.L. Klein, *J. Chem. Phys.* 79 (1983) 926-935.
- [40] (a) A. Onufriev, D. Bashford, D.A. Case, *J. Phys. Chem. B* 104 (2000) 3712-3720; (b) M. Feig, A. Onufriev, M.S. Lee, W. Im, D.A. Case, C.L. Brooks, *J. Comput. Chem.* 25 (2004) 265-284.
- [41] M.J. Mc Kennon, *J. Org. Chem.* 58 (1993) 3568-3578.
- [42] L.F. Tietze, C. Schneider C, A. Grote, *Chem. Eur. J.* 2 (1996) 139-148.

- [43] D. Zampieri, M.G. Mamolo, E. Laurini, M. Fermeglia, P. Posocco, S. Pricl, E. Banfi, G. Scialino, L. Vio, *Biorg. Med. Chem.* 17 (2009) 4693-4707.
- [44] I.T. Crosby, J.K. Shin, B. Capuano, *Aust. J. Chem.* 63 (2010) 211-26.
- [45] M. M. Bradford, *Anal. Biochem.*, 72 (1976) 248-254.
- [46] C. Stoscheck, *Methods in Enzymology* 182 (1990) 50-68.
- [47] Y. Cheng, H. W. Prusoff, *Biochem. Pharmacol.*, 22 (1973) 3099-3108.
- [48] D.L. De-Haven-Hudkins, L.C. Fleissner, F.Y. Ford-Rice, *Eur. J. Pharmacol. Mol. Pharmacol. Sect.*, 227 (1992) 371-378.
- [49] R.H. Mach, C.R. Smith, S.R. Childers, *Life Sci.*, 57 (1995) PL 57-62

**Highlights**

1. New 1-(4-(aryl(methyl)amino)butyl)-heterocyclic sigma-1 receptor ligands were designed by computer-aided technics and subsequently synthesized
2. Some of new derivatives showed high affinity and high selectivity for the sigma-1 receptor
3. In silico affinity predictions were confirmed by experimental data
4. We performed a preliminary functional assay in order to verify the cytotoxic effects of new synthesized derivatives
5. Compounds featuring a 4-phenyloxazolidin-2-one moiety displayed the best biological profile.